A review on numerical modelling of flashing flow with application to nuclear safety analysis

Liao, Y.; Lucas, D.;

Originally published:

September 2020

Applied Thermal Engineering 182(2021), 116002

DOI: https://doi.org/10.1016/j.applthermaleng.2020.116002

A review on numerical modelling of flashing flow with application to nuclear safety analysis

Yixiang Liao[a,*], Dirk Lucas[a]

[a]Helmholtz-Zentrum Dresden - Rossendorf, Institute of Fluid Dynamics, Dresden, Germany

---

Abstract

The flashing flow is an relevant multiphase phenomenon in many technical applications including nuclear safety analysis, which has been the subject of intense research. Numerical studies have evolved from one-dimensional to multi-dimensional. A variety of methods have been proposed, while a broad consensus was not exiting. The present work aims to present an overview of available models as well their assumptions and limitations by conducting a literature survey. The final focus was put on recent computational fluid dynamics simulations. Some consensus on modelling interfacial slip, phase change mechanism and bubble size is identified. Since flashing scenarios often accompanying with high void fraction and broad bubble size range, a poly-disperse two-fluid model is recommended. Thermal phase change model is superior to pressure phase change, relaxation and equilibrium models for practical flashing problems. Major challenges include improving closure models for interphase transfer, bubble dynamics processes, interfacial area as well two-phase turbulence. For this purpose, high-resolution high quality experimental data are important, which are lacking in many cases. Considering that heterogeneous gas structures often exist in flashing flows, multi-field approaches able to handle different shapes of gas-liquid interface are recommended.

Keywords: computational fluid dynamics, flashing flow, nuclear safety analysis, numerical modelling, literature review

*Corresponding author
Email address: Y.Liao@HZDR.de (Yixiang Liao)

1. Flashing phenomenon and its relevance to nuclear safety

Production of steam from water boiling is a familiar process under normal operation of light water nuclear reactors, for example, in the core of Boiling Water Reactors (BWRs) and in the Steam Generator (SG) of the Pressurized Water Reactors (PWRs). In these normal situations, water is heated to saturation temperature by a hot structure or heat source, e.g. fuel rods in the core or U-tubes in the SG, and steam as energy carrier drives the turbine generators to produce electricity. On the other hand, phase change from liquid to vapor can be triggered by depressurization under nearly adiabatic conditions. Pressure drop may occur in pipes with varying cross section and enhanced elevation, in relief valves, breaks or other types of mechanical failures[1]. The pressure-driven phase change can be considered as a spectrum of phase change phenomena with cavitation at the cold end and flashing at the hot end [2, 3]. In the case of hot liquids, the temperature of liquid remains almost constant till the phase change starts, but the saturation temperature drops with the pressure. As the pressure of the liquid reaches the saturation pressure corresponding to its temperature, boiling i.e. formation of vapour bubbles takes place as a result of interfacial heat transfer, but sometimes the pressure has to drop below the saturation point [2]. The bubble growth and vapor generation is predominantly controlled by the heat transfer rate at the liquid-vapor interface. The difference between the saturation pressure and the pressure at boiling inception is often referred to as pressure undershoot characterizing the maximal non-equilibrium between the liquid and vapor phases [4]. Its value depends on the initial temperature of liquid, depressurization rate, liquid and vapour properties as well nucleation sites available in the system. The thermally-controlled vaporization process under depressurization is commonly referred to as flashing in the community of nuclear engineering, but more often as flash evaporation in the field of desalination [5–8] and flash boiling in spray atomization [9–12]. The flashing phenomenon has received great interest from various branches, and a review on its application and consequence as well existing experimental, theoretical and numerical studies is given by [13]. Although many industrial processes benefit from the flashing phenomenon, for example, steam and spray generation [14, 15], absorption and oxidation [16, 17] as well as desalination for gaining drinking water [18–20], the fast phase change process may have a significant impact on the safety and performance of many devices and systems. Concerning nuclear safety analysis, flashing behavior is of key importance in terms of determining the reduction rate of reactor coolant inventory and affecting core thermal-hydraulics during the loss of coolant accident (LOCA), and inducing flow instabilities in passive safety systems driven by natural circulation.

1.1. Flashing-related topics under LOCA conditions

- **Critical flow problem**: In the frame of nuclear safety analyses numerous researchers have investigated steady-state flashing flows through pipes, nozzles, orifices and other restrictions in relation with critical flow problem [21, 22]. In such flows vaporization develops under a constant pressure difference between the inlet and exit of the pipe. As the exit pressure drops below a critical value, the flow rate doesn't increase anymore, which is referred to as critical (or chocked) flow. A large body of literature on both experimental and numerical studies arose in the period from late 1960s to early 2000s, e.g. [23–30] among many others. Most of the efforts are driven by the need of predicting maximal flow rates under critical conditions, since it determines the rate at which coolant inventory leaves the reactor cooling system in LOCAs. Among others the BNL (Brookhaven National Laboratory) experiments on flashing flow in a converging-diverging circular nozzle [26] have been analyzed in many numerical works, e.g. [31–41].

- **Pipe blowdown transient**: There have been also many experimental and theoretical works on transient two-phase flashing flows under pipe blowdown conditions. The major concern here is the early-stage response of initially subcooled but hot liquid in a pipe or vessel during sudden depressurization, including the change of fluid temperature and pressure as well as the inception of flashing and void development. The information is of importance for analyzing the system behaviour and checking over the action of safety and protection systems during the accident. Edwards and O'brien [42] performed transient blowdown experiment using a 4.09 m long 0.073 m diameter pipe. The horizontal pipe was filled with pressurized heated water, a glass disk at one end was ruptured to initiate the blowdown. The measurements of pressure at several positions as well as void fraction have been used for model validation in a number of numerical works such as [43–45]. Takeda and Toda [46] investigated the pressure behavior in a vertical pipe ruptured at the top end with an initial temperature gradient increasing from bottom to top. The case was analyzed by Lafferty et al.[47] and Costa et al.[48] with the RELAP5 and WAHA code, respectively. Similar blowdown experiments were conducted by Lienhard et al. [49], Bartak [50] and others. Instead of analyzing the transient pressure behavior in the tube, the objective of these studies was the study of the nucleation delay phenomenon. Semi-empirical correlations based on the classical nucleation theory and experimental data were derived for determining the pressure undershoot.

- **Lower plenum flashing**: Although the study of pipe critical flow and blowdown phenomena is a contributing part of the LOCA analysis, the fluid behavior and steam generation in the pressure vessel is as well of great interest in the nuclear safety analysis. It affects directly the core cooling and occurrence of core meltdown. As the downcomer level falls, the initially subcooled lower plenum may exceed saturated conditions and flash, resulting in a surge of two-phase flow upwards through the core to the upper plenum. This may reduce the liquid inventory in the lower plenum and downcomer because of vaporization and entrainment, and may also reduce the reflood driving head and prevent the injected cooling water from entering the downcomer. Nevertheless, the liquid entrained in the steam flowing toward the upper part of the vessel may often give a significant contribution to the cooling of uncovered fuel rods, both in PWR and BWR systems [51, 52]. Transient two-phase flashing flow in the core or large pipes relative to the phenomenon of counter-current flow limitation (CCFL) is investigated insufficiently, due to the complexity of the incident. Phenomenologically, the flashing effects observed in the lower plenum can also be encountered in control rod guide tubes. Because of different geometry and initial liquid subcooling, the flashing intensity is lower and thus less important than the previous one as far as nuclear reactor safety is considered. Nonetheless, it may affect the core thermal-hydraulic behaviour in a later stage of LOCA transients [51]. In comparison to pipe critical or blowdown flows mentioned above, investigation on the flashing process occurring inside the vessel is challenging due to the large geometry size as well as complex internals. A limited number of studies were performed in this area, and a few large-scale experiments on blowdown effects in the pressure vessels are available, e.g. [53–55]. Recently, Wang et al. [56] studied the two-phase flow instability in a PWR-type small modular reactor under LOCA conditions. The temperature and void fraction transients were measured at four ports in the core and riser, and the pressure drop between these ports as well as between the top and the bottom of the containment was measured through differential pressure drop transducers. Ylönen [57] reviewed existing experiments on large-break LOCA, and concluded that for the purpose of CFD code validation, suitable data such as pressure and void fraction at both axial and radial positions are needed.

- **SG tube rupture flashing**: In a PWR steam generator (SG) tubes constitute a large fraction of the reactor primary coolant loop pressure boundary. The SG tubes play an important safety role. Any leakage resulting from SG tube rupture (SGTR) will allow radiation to escape into the non-radioactive side of the plant and likely to environment, the function containment being bypassed [58]. Although the core melt frequency resulting from SGTR is low relative to other severe accidents, it is a major accident in the field of nuclear safety considering its direct impact on the environment. Coolant flow rate through the break is a key in the analysis of SGTR. Due to high pressure drop through the break, the coolant flashes rapidly and the flow becomes chocked or critical. As introduced above the critical flow problem has been a subject of intense study both experimentally and theoretically. However, the research in the past mostly focused on blowdown from vessels, large pipes or short nozzles, while SGTR presents a particular class of small-break LOCAs (SBLOCAs). The width of the crack is in the micrometer range and the length of flow path approximates the thickness of SG tube walls ($\sim 1mm$) [59]. Assessment and extension of numerical models is necessary. The overall system performance of a light water PWR during SGTR events with different number of ruptured tubes and with/without ECCS (Emergency Core Cooling System) was tested in many institutions [60–63].

1.2. Flashing-induced instability (FII)

Passive systems utilizing natural circulation have advantages over active ones, and are frequently adopted in new generation reactors [64]. The passive containment cooling system (PCCS) has been developed as an advanced safety feature, for example, in AP1000 [65], ESBWR[66], iPOWER [67], VVER-1200 [68], KERENA$^{\mathrm{TM}}$ [69], and the Hualong pressurized reactor 1000 (HPR1000) [70]. A major disadvantage of the passive systems is the low driving force, which can lead to instability and safety problems. Due to hydrostatic pressure drop in the riser of natural circulation loop, steam generation by flashing can take place. As the steam bubbles condense in cold parts of the loop, oscillation of flow rate, temperature and pressure can be observed, which is referred to as Flashing-induced instability (FII). The FII phenomenon was first observed by Wissler et al. [71] as they conducted experiments on an open natural circulation test loop. Since then, many researchers performed experimental studies on the phenomenon, and a majority part focused on the instability problem in BWR during start-up, e.g. [72–75]. At the start-up condition, the coolant may not reach saturation temperature in the core, where it is heated up, and remain single-phase due to low power. However, because of considerable decrease in coolant saturation temperature along the flow path, flashing can occur in the adiabatic section above the core, and lead to self-sustained flow oscillation in the loop. A flashing-driven passive moderator cooling system was developed at AECL for CANDU reactors. It was shown that the concept was feasible at normal operating power, but caused flow instabilities at low power [76, 77]. Similar phenomena were observed in the PCCS systems mentioned above. Recently, Cloppenborg et al. [78] investigated two-phase phenomena in the KERENA^{TM}-CCC (containment cooling condenser) natural circulation system on the GENEVA test circuit. The riser section is two times longer ($\sim 9m$) in comparison to other natural-circulation systems such as CIRCUS [72], equipped with high time and spatial resolution instrumentation for local void fraction and temperature distribution. Since the late 1980s, many researchers have analyzed the FII using numerical methods, and various analysis codes were adopted such as TRACG [79], FLOCAL [80], RELAP5 [81, 82] and MARS [64, 83]. Lim et al.[64] attempted to develop stability maps for FII using the MARS code. Due to high-frequency transients and complex two-phase processes, high-fidelity modelling of FII represents still great challenge and difficulty.

2. Widely-used numerical models for flashing flows

As aforementioned, a large body of literature exists on the numerical study of various flashing scenarios conducted with application to nuclear safety analysis. The simulations progress from one-dimensional to three-dimensional. The models range from simple empirical to mechanistic ones with different levels of sophistication. Concerning whether non-homogeneous non-equilibrium effects are considered, they fall into four main categories (a) homogeneous equilibrium model (HEM), (b) non-homogeneous equilibrium model (NHEM), (c) homogeneous non-equilibrium model (HNEM) and (d) non-homogeneous non-

Models	Features	Subcategory	Reference examples
HEM	equal velocity equal temperature		[84–89]
NHEM	unequal velocity equal temperature	slip ratio model	[27, 28, 84, 90]
		drift-flux model	[91, 92]
		two-fluid model	[21, 93, 94]
HNEM	equal velocity unequal temperature	empirical model	[28, 42, 95–100]
		relaxation model	[101–107]
		delayed equilibrium model	[108, 109]
		physically-based model	[31, 43, 110–112]
NHNEM	unequal velocity unequal temperature	drift-flux model	[30, 32, 102, 113]
		two-fluid model	[81, 114, 115]

Table 1: Overview of numerical models for flashing flows

equilibrium model (NHNEM). The term "homogeneous" here means equal velocities while "equilibrium" denotes equal temperatures of the liquid and vapor phases. The models in each category differ further in their treatment of the mechanical and thermal non-equilibrium and the applied constitutive models, see Table 1. A brief introduction of these models, and a review on representative one-dimensional numerical works are provided in this section, while three-dimensional simulations are discussed subsequently.

2.1. The HEM model

As the name suggests, the HEM model simplifies the two-phase flow to a pseudo or an equivalent single-phase one flowing with an average velocity and possessing mean thermodynamic properties, which are obtained by interpolating between the saturated liquid and vapour ones using the equilibrium quality. In order to use well-established single-phase theories, the HEM model was very often used for LOCA analysis around 1950s, for example, available in early versions of the system code RELAP. Among others Leung [116] presented a critical flow model on the basis of HEM assumptions. It works well for long pipes for example with a length exceeding 3.0 inches [84], where the time is sufficient for equilibration between the phases. Many works [84–87] discuss the difference between measured and predicted critical flow rates for short pipes, in which there is insufficient time for the two-phase mixture to proceed to equilibrium. The flow rates predicted by the HEM model are considerably less than those obtained experimentally. Deligiannis and Cleaver [112] found that the HEM model is incapable of predicting the earliest stage of a rapid depressurization, where the effect of nucleation and thermal non-equilibrium is of prime importance. Inada [88] and Van Bragt et al. [89] investigated flashing effects and instability mechanisms in a natural circulation BWR using the HEM model. Concerning the flow instability Hu et al. [117] and Podowski [118] reported that the HEM predictions are conservative in comparison with a slip or two-fluid model, because the HEM void fraction is higher. According to [29] in the initial stage of steady-state flashing, when bubbles are small and finely dispersed in the liquid, an assumption of hydrodynamic momentum equilibrium is applicable, however, thermal non-equilibrium has to be considered since the interfacial area available for heat transfer is very limited. As the bubbles grow and void fraction exceeds a value of 0.3, thermal equilibrium may be assumed but slip between the phases becomes important and ignoring it will cause inaccuracies.

2.2. NHEM models

Attou et al. [93] studied the effect of interfacial slip on bubbly flow through a sudden enlargement by analyzing two extreme conditions with maximum or negligible momentum transfer between the two phases, respectively. The former assumption is equivalent to HEM, while the latter was referred to as a momentum frozen model (MFM). It was found that in HEM, due to complete momentum transfer between the phases, the lower inertia of the gas causes the liquid to decelerate faster than in reality, leading to a higher pressure recovery than predicted in experiments. Consequently, the MFM causes the liquid to decelerate slower and hence the pressure recovery predicted is lower than in experiments. Addressing the finite rate of interphase transfers is of importance in analyzing flashing flows especially at the later stage [29]. Most earlier efforts have been devoted to developing empirical or theoretical correlations for the velocity (or slip) ratio. The theoretical models for critical flow presented in [27, 28, 84, 90] for long tubes are based on the thermodynamic equilibrium assumption but relax the requirement of equal phase velocities by introducing a slip ratio. The next level of complexity is to use the drift-flux model to characterize the effect of the relative motion, which evaluates the void distribution parameter and the vapor drift velocity pure empirically. Hu et al. [91] investigated the FII during a BWR reactor start-up using a NHEM model. The vapor generation rate was derived from the mixture energy conservation equation, while the nonhomogeneous velocities of the liquid and vapor was considered using the drift-flux approach. A similar equilibrium approach was used in [92] for the linear stability analysis of a boiling natural circulation loop. On the other hand, Wallis [21] and Bouré [94] disadvised the use of drif-flux models. They warned that the relative motion in a rapidly accelerating/decelerating flow with changing void fraction as well flow pattern is determined by a quite different set of terms from which the derivation of drift-flux correlations is based on. It is important to take into account the mechanical interaction between the phases using a separated flow model or two-fluid model when the flashing flow has to be modelled [93].

2.3. HNEM models

Similar to homogeneity of phase velocities, the validity of assumption about thermal equilibrium is limited. According to Donwar-Zapolski et al. [119], the most important feature of flashing flows is the thermal non-equilibrium effects caused by nucleation delay and limited rate of vapor generation. Flashing starts with some delay until the pressure drops below the saturation line, and the real quality pattern differs essentially from the equilibrium one. This greatly influences the void fraction as well as the pressure and velocity distribution along the flow. Kato et al. [120] presented an equation which gave the relative importance of inertial and thermal effects controlling bubble growth in superheated liquid. It was shown that the model has to capture the non-equilibrium nature of the flow in order to simulate flash boiling accurately [121]. The methods describing thermal non-equilibrium fall in four categories:

- Empirical models: The HEM model is known to over-predict the vapor generation rate and thus under-predict the flow rate in the critical flow. Henry and his co-workers [28] intended to consider the non-equilibrium effect by introducing a correction factor, which allows only a fraction of the equilibrium vapor generation to occur. The empirical factor was derived based on the deviation between the measured flow rate and the HEM prediction, and its expression largely depends on the pipe length to diameter ratio. For a slip ratio value of unity the authors presented a simple correlation being a function of equilibrium quality only. It assumes that if the quality exceeds 0.05 thermal equilibrium is achieved. For low qualities the non-equilibrium factor was set to 20 times the equilibrium quality, i.e. $N = 20x_{eq}$. The actual flow rate was estimated as $G_{HEM}/N^{1/2}$, where G_{HEM} is the flow rate obtained from the HEM model. In their homogeneous model assuming equal phase velocities, Simpson and Silver [95] and Edwards [42] introduced two empirical coefficients to account for the non-equilibrium nucleation process. One is the time-delay for bubble nucleation, and the other is the number concentration of bubble nuclei. For sake of simplicity Lackmé [96] assumed that evaporation should start if the pressure falls about 5% below the saturation pressure. To determine the nucleation delay more reliably, many experimental and theoretical works on the determination of pressure-undershoot have been carried out, e.g. [4, 50, 97, 98] among others. Based on the classical homogeneous nucleation theory and measurement of pressure-undershoot, semi-empirical correlations were proposed, which have been frequently used in the one-dimensional analysis of flashing critical flows such as [99, 100]. A brief summary of such models as well their applications was given in [2, 122].

- Relaxation models: The basic idea of the relaxation model is that the actual quality x is lower than the equilibrium one x_e. It increases proportionally to the difference between them during the flashing process. The relaxation model for LOCA analysis was first discussed in [101, 102], where the vapor generation rate is correlated with $x_e - x$. Bilicki and Kestin [103] proposed the homogeneous relaxation model (HRM) by adding a rate equation to the HEM equations. It describes the rate of the actual quality x approaching its local equilibrium value. The necessary coefficient is the relaxation time, which is a function of system pressure, mixture enthalpy and actual quality. Downar-Zapolski et al. [119] derived a correlation for the relaxation time basing on the "Super Moby Dick" experiments on critical flow rates [23]. It is a monotonically decreasing function of void fraction and the non-dimensional pressure difference $(p_{sat}(T_{in}) - p)/p_{sat}(T_{in})$. The HRM model and the relaxation time correlation of [119] has been widely adopted in the computational fluid dynamics modelling of flash-boiling atomization, e.g. [3, 104–107], while less in the nuclear safety analysis. Similar relaxation times may be derived for other thermodynamic parameters, and they may differ. Bilicki et al. [123] presented a method for the evaluation of the relaxation time of interphase heat exchange. Mohammadein [124] derived a formula for the thermal relaxation time by solving energy and relaxation equations analytically, in terms of two-phase mixture between two finite temperatures boundaries.

- Delayed Equilibrium Model (DEM): In comparison to others, the delayed equilirium model (DEM) is not widely used. For the sake of completeness, it is introduced briefly here. The basic idea of the DEM for describing the flashing flow is that the mixture is composed of three phases, i.e. saturated liquid, saturated vapor and metastable liquid [108]. The third phase is in thermal non-equilibrium with the saturated ones, while the whole mixture is at pressure and mechanical equilibrium. The expansion of the metastable liquid is an isentropic process. In addition to the mixture system of equations, an extra mass balance equation for the metastable liquid phase is solved. De Lorenzo et al. [109] benchmarked the DEM model and other three well-known two-phase critical flow models, namely, the HEM model, the Moody NHEM model [27] and the Henry-Fauske HNEM model [28], against more than 450 experimental data. The results showed that none of the classical models can be considered as a general method for the evaluation of the two-phase critical flow. Although positive results in evaluating the critical mass flow rate of long tubes, HEM fails in predicting the critical pressure. Moody's model is unsuitable under two-phase stagnation conditions. The Henry-Fauske model provides rather good results for nozzles and orifices, but overestimates the critical mass flow in long tubes. On the other hand, DEM exhibits reliable results for the configurations ranging from long and short tubes to narrow slits in terms of both critical pressure and critical mass flux.

- Physically-based models: As aforementioned, thermal non-equilibrium processes in a flashing flow concern nucleation and interphase heat transfer. Some works consider both of them, while others only the latter by prescribing a constant bubble number density. Despite numerous attempts have been made, limited understanding of the physical phenomena prevent from defining the non-equilibrium effects precisely. So, it can happen that the results obtained from a physically-based model are worse than those from a simpler one [21, 125]. The non-equilibrium models can be incorporated with homogeneous, drift-flux or two-fluid models in one or more spatial dimensions. Within the context of a one-dimensional homogeneous model, Wolfert et al. [43] simulated three blowndown experiments by focusing on the interphase heat transfer, which determines the vapor generation rate. The overall transfer coefficient was calculated by combining the heat diffusion model of Plesset and Zwick [126] and the convection model of Ruckenstein [127] cumulatively. Furthermore, they took into account the turbulence enhancement by introducing an eddy conductivity. The bubble number density was treated as a constant, needed to be adjusted from case to case. For the modelling of flashing flow in a converging-diverging nozzle, Wu et al. [31] attempted to find out the flashing inception location by using the semi-empirical onset correlation of Alamgir and Lienhard [4]. Downstream from the onset location, a constant number of bubbles was assumed, and the bubbles initially have the critical size corresponding to the onset pressure. The vapor generation rate was assumed to be limited by heat conduction and calculated from the correlation proposed by Plesset and Zwick [126]. The lack of understanding of the heterogeneous nucleation process remains one difficulty in the modelling of flashing flows. Rohatgi and Reshotko [110] simulated flashing liquid nitrogen flow in a venturi using a one-dimensional HNEM model. They accounted for heterogeneous nucleation by making analogy to the classical homogeneous nucleation theory with the assumption that nucleation in the bulk is dominant. Two adjustable parameters are contained in their model, one being the value of activated nucleation site density and the other being the heterogeneity factor. Blinkov and his co-workers developed a quasi-one-dimensional HNEM model to calculate the behavior of nucleation and flashing in nozzles [111]. Besides the mixture conservation equations, one continuity equation for the vapor phase and one transport equation for the bubble number density were solved. Both bulk and wall nucleation phenomena were considered. Heterogeneous nucleation in the bulk was modelled by assuming a size distribution of pre-existing nucleation sites, and the activated nucleation site density is correlated with the Gibbs number. A cavity model was proposed for determination of the nucleation site density, bubble departure diameter and frequency at the wall. Deligiannis and Cleaver[112] considered the effect of homogeneous and heterogeneous nucleation in the frame of a two-fluid model with zero slip between the phases.

2.4. NHNEM models

Besides above homogeneous models, the non-equilibrium effects regarding nucleation and interphase heat transfer are often considered in the context of non-homogeneous models, where the velocity difference between the gas and liquid phases is taken into account by using the drift-flux or two-fluid model. [30, 32, 102, 113]

- Drift-flux model: Kroeger [102] applied a non-equilibrium drift flux model to two-phase blowdown experiments. The vapor generation rate was calculated from a relaxation type model, and the vapor drift was considered by the correlations proposed by Zuber and Findlay [128]. Another non-equilibrium drift flux model was presented in Elias and Chambé [113]. They assumed that the evaporation rate is governed by interphase heat transfer. The evaporation rate is determined by a conduction bubble growth model[129], while the convection effect is negligible. A similar non-equilibrium model was developed by Saha and his co-workers [30], and the major difference lies in modelling of interphase heat transfer. Saha et al. stated that the Plesset-Zwick or Forster-Zuber type of heat transfer coefficient may be applicable for short time after nucleation. As the bubbles "age", convection starts to dominate the heat transfer because of the relative velocity between the bubbles and liquid. They used a simple expression which provides the root mean square of the conduction and convection heat transfer coefficients [130]. Riznic et al.[32] improved the drift-flux model by considering bubble generation and transportation instead of assuming a constant bubble number density. The bubble number transport equation was solved with a distributed source from wall nucleation. In addition, they took into account the variable pressure effects in their conduction bubble growth model according to the results of Jones and Zuber [131]. They found that in a variable pressure field, which cause the saturation temperature to vary as t^n (t being time), the bubble radius will grow as $t^{n+1/2}$. It is significantly faster than $t^{1/2}$ usually expected for the initial superheat.

- Two-fluid model: Saha et al.[30] recognized that a two-fluid model is superior to the drift-flux model for calculating relative velocity. One-dimensional two-fluid equations were used by Ardron [132] for the calculation of critical flow in a pipe. The nucleation and diffusion-limited growth of vapor bubbles in superheated liquid were considered in the determination of vapor generation rate. The nucleation rate was computed based on the classical nucleation theory by introducing a heterogeneity factor. A similar model was presented in [110], where the density of nucleation sites and the heterogeneity factor are two adjustable parameters. By neglecting the sphericity of the bubble and assuming linear time variation of the liquid superheating degree, the diffusive heat flux from the thermal boundary to the bubble wall was approximated as

$$q_i(t,t') = \frac{\lambda_l}{\sqrt{\pi a_l (t-t')}} \left[2T_{sup}(t) - T_{sup}(t')\right] \tag{1}$$

  where t' is the time point at which the bubble is created, λ_l abd a_l are liquid thermal conductivity and diffusivity. Rivard and Travis [133] described the vapor production and bubble growth by the well-known heat diffusion controlled rate presented in [126], but considered the enhancement in thermal diffusivity due to the effect of relative motion and liquid turbulence, i.e. $a_{eff} = a_l + A r_B U_{rel}$, where $a_{eff}, a_l, r_B, U_{rel}$ is effective diffusivity, molecular diffusivity, bubble radius and relative velocity, respectively, and A is an empirical constant. In addition, a constant bubble number density $N = 10^9 m^{-3}$ was specified and nucleation was neglected. Richter[29] applied the two-fluid model to calculation of critical flow rates for steam-water mixtures from nozzles. He postulated that convection is the dominant mode of interphase heat transfer during flashing, and adopted the empirical correlation proposed by Ranz and Marshall [134] for estimation of heat transfer coefficient in the bubbly flow regime. Different flow regimes were considered in the model, like bubbly, churn-turbulent and annular. The transition from one regime to another was assumed to occur at certain void fractions. A similar two-fluid model was presented in [125], while different correlations were used for the constitutive equations, i.e. drag coefficient and heat transfer coefficient. Schwellnus [135] included a seventh equation for bubble diameter up to the point from bubbly to churn-turbulent flow. The bubble number density was updated basing on the bubble diameter and void fraction. For the purpose of analyzing critical flows in pipes of nondiverging cross-sectional area, Dagan et al. [136] derived an empirical correlation for the number density of bubbles as a function of pipe's length to diameter ratio. Furthermore, they extended the conduction bubble growth model proposed by Olek et al. [137] to include the convection effects. Tiselj and Petelin [33] simulated the critical flashing flow in a converging-diverging nozzle with the two-fluid model in RELAP5. The simulation results were compared with the experiments performed in the BNL laboratory [26]. They pointed out that the major source of discrepancies is the neglect of the flashing delay. Recently, Kozmenkov et al. [81] and Atajafari et al. [114] validated the RELAP5 code for FII observed at the CIRCUS [72] and SIRIUS-N [73] test facilities , respectively. Wein [115] developed a two-fluid model for flashing flows of initially subcooled and saturated fluids through pipes and nozzles. It consists of six conservation equations of mass and momentum, liquid thermal energy and bubble number transport. Constitutive equations describing interphase mass, momentum and heat transfer account for different flow regimes. Nucleation on the wall and in the bulk flow was considered. The results proved that the importance of fluid dynamic non-equilibrium increases with vapor volume fraction.

3. Computational fluid dynamics modelling

Multi-dimensional CFD-based simulations are becoming a useful tool for studying transients, instabilities and phase transitions in two-phase flow sys-

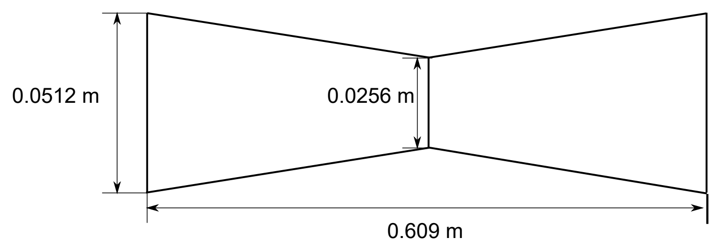

Figure 1: Vertical circular convergent-divergent nozzle in BNL experiments [26]

tems [118]. Since the beginning of the 2000s there arise a number of CFD works on flashing flow related to the nuclear reactor safety problems. Insights to smaller scale flow processes which were not seen by system codes may be acquired by using the CFD tool. It brings a better understanding of local physical phenomena, more confidence in the results and then better definition of safety margins. However, the same problem as in one-dimensional codes encountered here is that, constitutive models are not as mature as in single phase flows, and a general consensus regarding model selection is not available. A lot of work has still to be done on the physical modelling and numerical algorithm [138].

3.1. Flashing nozzle flow

CFD simulation of flashing flows in nuclear applications are mostly concentrated on the steady-state nozzle flow or critical (chocked) flow. Considering that the BNL experiments [26] have been frequently simulated, geometrical details about the nozzle and some test runs are presented in Figure 1 and Table 2, respectively. In most cases the mass flow rates obtained using different models conform well with the data, although adjustment of some parameters such as the accommodation coefficient [41] and the bubble number density [40] was often necessary. Details about the numerical methods and models adopted in each work are discussed below.

Maksic and Mewes [35] examined the flashing flow in the BNL nozzle [26] by performing simulations with the commercial CFD-code ANSYS CFX version 4.2. The simplified two-phase model consists of continuity and momentum equa-

Run #	p_{in} [kPa]	p_{out} [kPa]	T_{in} [K]	$\dot{m}_{exp}$ [kg/s]	$\dot{m}_{cal}$ [kg/s]
122	171.0	109.2	373.35	6.12	6.25 [36]
128	248.0	101.0	373.15	9.13	8.78 [36]
133	349.0	203.0	394.35	9.0	9.2 [40] 8.80 [36]
137	464.0	208.9	394.75	11.95	12.1 [40]
145	306.0	208.7	394.35	7.52	7.7 [40] 7.37 [37]
148	304.0	206.0	394.35	7.52	7.50 [36] 7.33 [37]
268	575.2	443	422.05	8.74	8.4 [40] 9.20 [41] 9.10 [139]
273	573.5	442.1	421.85	8.72	8.3 [40], 8.85 [35] 8.51 [37], 9.30 [41]
278	688.6	434.1	421.95	11.67	10.9 [40], 12.30 [41]
284	530.1	456.0	422.35	7.30	7.0 [40], 7.70 [41]
288	530.8	456.3	422.25	7.26	7.12 [37]
291	504.7	470	422.05	6.44	6.1 [40]
296	764.9	432.6	421.95	13.13	12.4 [40], 13.90 [41]
304	577.7	441	422.15	8.76	9.1 [40], 9.10 [41]
309	555.9	402.5	422.25	8.80	8.4 [40], 8.75 [36] 7.56 [37], 8.80 [41] 8.72 [139]
344	539.9	190.0	394.15	13.47	12.7 [40]
348	226.9	199.4	394.35	4.57	4.30 [37]
358	370.2	101.2	373.15	12.13	11.5 [40]
362	443.3	101.2	372.85	13.68	12.9 [40]

Table 2: Operational conditions and test runs in BNL experiments [26]

tions for the mixture of liquid and vapor, a separate continuity equation for the vapor and an energy equation for the liquid. The vapor phase was assumed to be saturated, and its temperature was calculated from the local pressure. The four-equation HNEM model was supplemented with a transport equation for the bubble number density. Both bubble sizes and numbers were allowed to change in this way. The generation of bubbles from wall nucleation was considered, and the nucleation rate was calculated according to the Jones model [111, 131]. The surface source was transformed to a volumetric source by multiplying it with the ratio of the pipe perimeter to the cross-sectional area of the pipe $\frac{\xi}{A}$, i.e.

$$J_w = N_w f_w \frac{\xi}{A} \tag{2}$$

where N_w, f_w denotes the nucleation site density and nucleation frequency at the wall, respectively. The transformation in Eq. (2) may lead to inconsistency, since N_w has a value of zero everywhere except in the cells adjacent to the wall. For the calculation of interfacial area density, the authors considered two regimes, bubbly regime ($\alpha < 0.3$) and slug regime (($\alpha > 0.3$)). In the slug flow regime, the interfacial area density was assumed to be the sum of that of spherical bubbles and cylindrical slugs, but the volume fraction of each type of the bubbles was not provided. The interfacial heat transfer was assumed to be dominated by heat conduction, and the Nusselt number is a function of the Jakob number. The empirical correlation presented by Labuntzov [140] was adopted.

$$Nu = 2 + \frac{12}{\pi} Ja + \left(\frac{6Ja}{\pi}\right)^{1/3} \tag{3}$$

The Jakob number is defined by

$$Ja = \frac{c_{pl} \rho_l \Delta T_{sup}}{\rho_v H_{lv}} \tag{4}$$

where c_{pl} is the isobaric heat capacity of liquid. For the test run 273 with inlet pressure of 573.5 kPa, temperature of 421.85 K, see Table 2, a good agreement on the mass flow rate was achieved. However, the simulation showed a fluctuating pressure profile in the diverging part of the nozzle, and under-predicted the void fraction in the diverging part of the nozzle.

Marsh and O'Mahony [37] simulated the same nozzle flow using a full two-fluid model in the commercial CFD code ANSYS FLUENT, with separate mass, momentum and enthalpy balance equations for liquid and vapour. Inter-phase mass and momentum as well as energy transfer resulting from both nucleation and phase change were taken into account. However, the effect of non-drag forces on the momentum exchange and heat transfer between the vapor and vapor-liquid interfaces were neglected. Like in the previous work vapor generation is determined from interphase heat transfer, but information about the heat transfer coefficient is not provided. The generation of bubbles from nucleation was taken into account by solving a bubble transport equation. The nucleation rate was computed by a modified version of the Blander and Katz model [141].

$$J_w = N^{2/3} S \left(\frac{2\sigma N_A}{\pi m_w B} \right)^{1/2} exp\left(-\frac{\phi}{(T_{sat} - T_l)^n} \right) \tag{5}$$

where N is the number of liquid molecules per unit volume, and the power 2/3 is to transform it to a surface density, m_w is the molecular weight and $S = (1 - m_w)/2$, N_A is the Avogadro number, σ is the surface tension coefficient, and B is a constant having a value of 2/3 in case of flashing. The exponential term was written in terms of superheat instead of pressure undershoot as in the original model for the sake of numerical stability. In addition to the heterogeneous factor ϕ an adjustable constant n was introduced. Details on how to convert the surface flux J_w to the volumetric source required by the bubble transport equation are not provided. The calculated and measured mass flow rate was compared for six BNL runs carried out by Abuaf et al. [26], see Table 2. Good agreement was achieved for all cases except Run 309, which has a high inlet pressure and a relatively low outlet pressure, in other words high vaporization rate. Furthermore, in contrast to that a bubble layer in the vicinity of the wall as reported in [35], the distribution of vapor in the diverging part of the nozzle is almost uniform. The difference mainly results from the nucleation models that are applied. The model of Blander and Katz [141] was derived from the classical nucleation theory for bulk nucleation and activated not only on the walls but all over the domain depending on local liquid superheat. It differs in nature from the Jones wall cavity model [111] used in the previous work.

The disagreement on nucleation modelling motivated Janet et al. [39] to evaluate the existing models. They analyzed the heterogeneous nucleation effects in the BNL nozzle using the two-fluid model in ANSYS CFX 15.0. As in the work of Maksic and Mewes [35], the vapor and vapor-liquid interface were assumed to remain saturated by applying the zero resistance model, but separate velocity fields were solved for the liquid and vapor phases. To estimate the heat transfer between the superheated liquid and the interface, the correlation of Aleksandrov [142] was used. It combines the heat diffusion and convection in the following way:

$$Nu = \left(\frac{12}{\pi^2} Ja_T^2 + \frac{1}{3\pi} Pe\right)^{1/2} \tag{6}$$

where Pe is the Péclet number. Like in [35, 37] a transport equation was solved additionally for the bubble number density. The nucleation source was implemented as a boundary flux into the near-wall mesh cells. Three wall nucleation models, i.e. the Jones model [111, 131], the RPI model [143] and Riznic model [32], were investigated. The performance of the models was found to differ qualitatively and quantitatively in predicting of the bubble departure frequency and diameter along the nozzle. The Jones model predicted the best agreement on the mass flow rate. Considering only wall nucleation leads to the same profile as observed in [35], i.e. a bubble layer appearing in the vicinity of the wall, whose thickness increases along the nozzle axis, while the void fraction in the central part of the nozzle is nearly zero. On the other hand, the measured profiles show non-zero values in the central region along with high peaks near the wall. Based on this observation, Janet et al. [39] suggested that both wall and bulk nucleation play a role in flashing nozzle flows although wall nucleation is dominant in most cases. The effect of bulk nucleation was considered by using the model proposed by Rohatgi and Reshotko [110]. The bulk nucleation rate is given by

$$J_b = N_b \left(\frac{2\sigma}{\pi m_w} \right)^{1/2} exp \left(-\frac{16\pi\sigma^3\phi}{3\kappa T_l (p_{sat} - p_l)^2} \right) \tag{7}$$

where N_b is the number density of liquid molecules, p_{sat} is the vapor pressure at the liquid temperature and κ is the Boltzmann constant. Considering both wall and bulk nucleation improves the agreement between the measured and simulated radial profiles considerably.

The nucleation region in above BNL nozzle test runs has been shown sufficiently narrow (a few centimeters) both experimentally [31] and numerically [39]. The bubble number density is nearly constant after the nucleation region. Based on these observations Liao and Lucas [40] revisited these cases with prescription of the bubble number density. The initial tiny bubbles can be deemed as pre-existing germs, which start to grow as long as the surrounding liquid becomes saturated. This is a major difference from the numerical model applied in the previous work of [39], where the nucleation delay was considered. Fourteen cases with different inlet/outlet pressures and temperatures were benchmarked. The error between predicted mass flow rates and experimental data for all cases was below 7%, see Table 2. At the same time, satisfying agreement regarding axial profiles of void fraction and pressure was observed, which are greatly improved in comparison with the one-dimensional results published in [31]. However, the lateral distribution of bubbles reveals large discrepancy, although non-drag forces including lift, added mass, turbulence dispersion and wall lubrication are considered [144]. Both simulation and experiment gives a wall-peak profile, but the predicted void fraction in the central region is much too high. It evidenced that dynamic processes such as bubble nucleation, growth, coalescence and breakup were not reproduced by the numerical model appropriately, apart from the uncertainties in the force models. To capture the lateral bubble migration, a poly-disperse approach tracing the local bubble size change is necessary.

Mimouni et al. [145] simulated one critical flow case of the Super Moby

Dick experiment [146] with the NEPTUNE_CFD solver. It has the boundary conditions of 39.96 bars at the inlet and 23.176 bars at the outlet, and the initial water subcooling is of about 10^oC. Mass, momentum and energy balance equations are solved for both liquid and vapor. The interfacial transfer of momentum consisted of three forces, i.e. drag, virtual mass and the secondary momentum source associated with the interfacial mass transfer. Nucleation occurring at the wall and pre-existing germs are considered. The former is modelled by using the Jones nucleation model [111], while the latter by presuming an initial void fraction. In addition, the original correlation for the nucleation site density was modified for sake of generality. The change of bubble size and number density was not solved, and instead, a constant value was prescribed for the bubble size. The heat transfer coefficient on the vapor side was set to a large value to ensure the vapor temperature remaining very close to the saturation temperature, and on the liquid side was calculated using the Ranz-Marshall correlation [134].

$$Nu = 2.0 + 0.6Re_p^{1/2}Pr_l^{1/3} \tag{8}$$

While the majority of investigations indicated that the wall nucleation is predominant in flashing flows, Mimouni et al. [145] found the vapor generation at the wall negligible in comparison to that from pre-existing nuclei. The inconsistency is caused by the fact that the pre-existing nuclei are activated earlier (at saturation conditions) and suppress the activation of nuclei on the walls. It can be expected that the void fraction in the central region would be over-predicted as shown in [40]. The effect of initial void fraction as well bubble size was discussed. Taking into account the poly-dispersity was identified as one important issue requiring further efforts.

In all above investigations phase change was deemed driven by thermal difference, and the bubble growth and vapor generation rate was determined by modelling the interfacial heat transfer process. Similar for nucleation models, a broad consensus on choosing interphase heat transfer models does not exist. In some works conduction was assumed to be a predominant heat transfer mechanism, while in others convection. An evaluation of the heat transfer coefficient models for flashing flows was conducted by Liao and Lucas [130]. They attempted to generalize the model by taking into account convection and turbulence effects along with the conduction, and validated it for condensing and evaporating flows [130, 147].

On the other hand, a few CFD works on the flashing nozzle flow assumed that phase change is controlled by pressure difference, and applied a conventional cavitation model derived from the R-P (Rayleigh-Plesset) equation. For example, Palau-Salvador et al. [36] simulated the BNL nozzle flow [26] using the cavitation model of Singhal et al. [148] available in the CFD code ANSYS FLUENT 6.1. The model assumes that the flow is isothermal. Pre-existing germs start to grow as local pressure drops below the saturation pressure, and collapse in the reverse case. Mass and momentum balance equations are solved for the mixture of liquid and vapor. Like in [35], a transport equation was solved for the vapor fraction besides the mixture conservation equation, and the source terms representing bubble growth and collapse are described by the R-P equation.

$$\dot{\Gamma} = \begin{cases} C_{vap} \dfrac{\max(1.0, \sqrt{k})(1 - f_v - f_g)}{\sigma} \rho_l \rho_v \sqrt{\dfrac{2(p_v - p)}{3\rho_l}} & \text{if } p \leq p_v \ , \\ -C_{cond} \dfrac{\max(1.0, \sqrt{k}) f_v}{\sigma} \rho_l \rho_l \sqrt{\dfrac{2(p - p_v)}{3\rho_l}} & \text{if } p > p_v . \end{cases} \tag{9}$$

Wherein f_v, f_g are mass fraction of vapor and non-condensable gases, k is turbulent kinetic energy, C_{vap}, C_{cond} are two empirical coefficients having a unit of m/s. The local turbulence effect on the saturation pressure is considered by considering an additional turbulent fluctuation:

$$p_v = p_{sat} + 0.195\rho k \tag{10}$$

Five BNL test runs from [26] were validated, see Table 2. Good agreement between the measured and calculated mass flow rates was achieved with a difference less than 4%. Satisfying prediction of axial pressure and vapor fraction was shown for one case, where the thermal non-equilibrium effect at the onset of flashing is not that significant. As expected from the homogeneous mixture model, the contour plot of void fraction exhibits a uniform distribution of vapor in the lateral direction of the nozzle, which is inconsistent with the experimental observation as discussed above. Another cavitation model in the ANSYS FLUENT code, i.e. the Schnerr and Sauer model [149], was utilized by Ishigaki et al. [150] for analyzing the two-phase critical flow in nozzles and breaks. The Super Moby Dick experiment [146] and the SGTR experiment at Large Scale Test Facility (LSTF) of Japan Atomic Energy Agency [151] were simulated. The authors concluded that the CFD code ANSYS FLUENT has the possibility for simulation of two-phase critical flows related nuclear safety analysis. The physical properties were shown to have a significant influence on the flow rate predictions, and an more accurate estimation is necessary. The authors treated the vapor as an ideal gas, and calculated the density of liquid according to the Tait equation of state. In contrast, the simulations performed in ANSYS CFX mostly use the IAPWS-IF97 formulation of the thermodynamic properties of water and steam.

On the other hand, Liu et al. [38] pointed out that above isothermal cavitation models cannot be used for flashing flows directly, because the dependency of vapor generation rate on temperature variations is usually non-negligible under the high temperature and pressure conditions. They constructed a so-called thermodynamic cavitation model based on the homogeneous multiphase model with common flow fields shared by all fluids including temperature and turbulence. In order to take into account the thermal effects in flashing, the dependency of fluid physical properties on the temperature was introduced, e.g. the saturation vapor pressure, surface tension as well liquid and vapor densities, using empirical formulas. The mass transfer source terms related to bubble growth and collapse were derived based on the H-K (Hertz-Knudsen) formula, which gives the evaporation-condensation flux based on the kinetic theory on a flat interface.

$$\dot{\Gamma} = \begin{cases} F_{vap} \dfrac{6(1-f_v-f_g)}{d_B} \dfrac{2\sigma}{2-\sigma} \sqrt{\dfrac{M}{2\pi RT}} (p_v - p) & \text{if } p \leq p_v \ , \\ -F_{cond} \dfrac{6 f_v}{d_B} \dfrac{2\sigma}{2-\sigma} \sqrt{\dfrac{M}{2\pi RT}} (p - p_v) & \text{if } p > p_v . \end{cases} \tag{11}$$

where M is the molar mass of liquid, R is the gas constant, T is the mixture temperature, and F_{vap}, F_{cond} are two adjustable constants. The contribution of turbulent fluctuation to the pressure variation was considered according to Eq. (10). The authors simulated one BNL nozzle test run with the modified cavitation model, and compared the simulation results with those presented in [36]. A minimal improvement of the axial void fraction profile was indicated. Furthermore, it showed surprisingly that the vapor volume fraction at the temperature of $100^o C$ is higher than $150^o C$. It implies that the way how the thermal effect was considered is inappropriate.

Le et al. [41] investigated the BNL nozzle flow experiments by implementing a similar model as [38] in the commercial code ANSYS FLUENT 16.2. The source term for the mass flux at the interface is derived according to the H-K formula,

$$\dot{\Gamma} = A_i \beta \sqrt{\frac{M}{2\pi R T_{sat}}} (0.195 \rho k + p_{sat} - p*) \tag{12}$$

where β is the so-called "accommodation" coefficient taking into account the thermal non-equilibrium effects partially. The interfacial area density A_i is modelled by assuming a constant bubble number density as in [40]. The source term was inserted by means of a user-defined function. The coefficient β as well the pressure difference $dp = p_{sat} - p*$ was treated as adjustable constants in the simulation. The model was validated against experimental data [26] and numerical results of previous work [39, 40]. The discrepancies between the measured and simulated radial vapor profiles were attributed to the two-phase mixture approach and the slip model, which makes use of an algebraic slip relation for the relative velocity. A two-fluid model along with a complete modelling of the thermal effects was recommended.

In the frame of a homogeneous mixture model Jin et al. [139] included source and sink terms of interfacial mass transfer induced by both pressure and thermal difference ($\dot{\Gamma} = \dot{\Gamma}_p + \dot{\Gamma}_T$). The pressure phase change model has a similar form as Eq. (11) and Eq. (12), i.e.

$$\dot{\Gamma}_p = \begin{cases} F_{vap}\dfrac{\rho_v f_l}{t_{ch}} min\left(1, \dfrac{p_v - p}{k_p p_v}\right) & \text{if } p \leq p_v \ , \\ -F_{cond}\dfrac{\rho_v f_v}{t_{ch}} min\left(1, \dfrac{p - p_v}{k_p p_v}\right) & \text{if } p > p_v . \end{cases} \tag{13}$$

where t_{ch} is the characteristic flow time, k_p is a scaling constant that determines the pressure level at which the vaporization model comes into effect. The thermal mass transfer rate was calculated according to the thermal phase change model presented by Lee [152].

$$\dot{\Gamma}_T = \begin{cases} F_{vap}\dfrac{\rho_l f_l}{t_{ch}} \dfrac{(T - T_v)}{T_v} & \text{if } T > T_v \ , \\ -F_{cond}\dfrac{\rho_v f_v}{t_{ch}} \dfrac{(T_v - T)}{T_v} & \text{if } T \leq T_v . \end{cases} \tag{14}$$

The model was implemented in a in-house CFD code, whose capability of simulating flashing flows was assessed by studying the BNL nozzle flow. Two test runs (309 and 268) were simulated, and good agreement in terms of axial profiles of pressure and void fraction was achieved.

Schmidt et al. [3] extended the classical one-dimensional closures for the HRM model proposed by Downar-Zapolski et al. [119], to multiple dimensions, and implemented them in the open source CFD code OpenFOAM. The solver was firstly validated for a case taken from Tikhonenko et al. [153], who explored flashing critical flow in various pipes with a sharp inlet. These experiments include pressure measurements along the length of the pipe. High-pressure and low-pressure correlations for the relaxation time Θ were tested.

$$\Theta = \begin{cases} 6.51 \times 10^{-4} \alpha^{-0.257} \psi^{-2.24} & \text{if } p \leq 10\text{bar} \ , \\ 3.84 \times 10^{-7} \alpha^{-0.54} \phi^{-1.76} & \text{if } p > 10\text{bar}. \end{cases} \tag{15}$$

where the definitions for ψ and ϕ are

$$\psi = \left| \frac{p_{sat} - p}{p_{sat}} \right| \tag{16}$$

$$\phi = \left| \frac{p_{sat} - p}{p_c - p_{sat}} \right| \tag{17}$$

where p_c denotes the critical pressure. Both correlations were found to under-predict the flashing rate, and the low-pressure correlation is especially far off. The second test case was taken from the experiments conducted by Fauske [154], in a relatively short and small tube. In this case, surprising good agreement on the mass flow rate was achieved by the low-pressure correlation, while the high-pressure correlation under-predicted by a factor of two. The authors concluded that future development should focus on developing a general correlation for the relaxation time, and considering non-homogeneous, turbulence and nucleation effects.

Similar attempts extending a one-dimensional model to multi-dimensions were made by Duponcheel et al. [155]. They implemented and the DEM model in the NEPTUNE_CFD multi-field solver, and tested it for flashing chocked flows. The validation cases were taken from the Super Moby Dick experiments [146]. Two inlet conditions were simulated: $T_{in} = 240.5\ ^oC$ and $T_{in} = 249.4\ ^oC$. The homogeneous condition, i.e. identical velocities for all the phases, is obtained by adding very large drag forces. The saturated liquid and vapor were constrained to remain saturated by adding strong interfacial heat transfer terms. The metastable liquid phase was considered "frozen", and no interfacial heat transfer with the saturated phases. The mass transfer from the metastable liquid to the saturated liquid was determined by using an empirical correlation. The implemented model was able to give good agreement for the case closer to saturation, but under-predicted the mass flow rate by 13.5% in case of larger inlet subcooling. Yet, in both cases the multi-dimensional results are worser than the one-dimensional ones using the original DEM.

As shown above various phase-change models have been adopted for the pre-

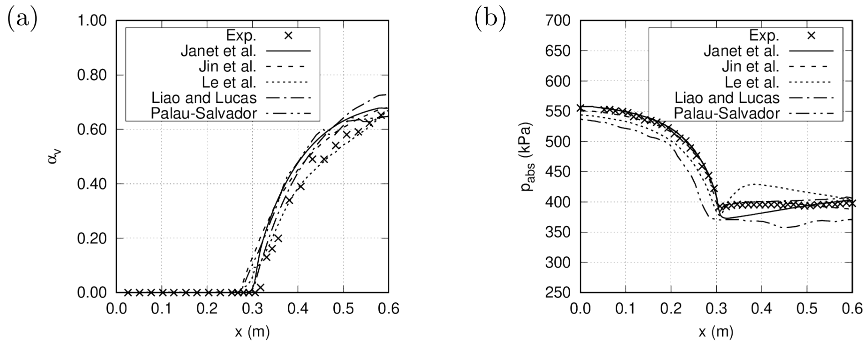

Figure 2: Comparison between simulation results from literature for BNL test case 309 [4]. (a) Axial void fraction profile (b) Axial pressure profile

diction of flashing flows, e.g. thermal phase-change model based on temperature difference (TPCM) and pressure phase-change model based on pressure difference (PPCM). The PPCM models can be divided further into two categories, i.e. based on the kinetic theory of gases (H-K equation) and based on bubble dynamics (R-P equation). A comparative evaluation of these models was performed by Karathanassis et al. [156] together with the two-phase mixture model in ANSYS FLUENT 14.5. The results showed that the phase-change model based on the kinetic theory of gases produced accurate predictions for all the cases investigated ("Super Moby Dick" nozzle [23], "Reitz" nozzle [157], "Edwards" pipe blowdown [42]), while the validity of HRM and model based on the R-P equation was found situational. Similar results were presented in [158], which showed that the PPCM model based on the R-P equation failed in reproducing the pressure undershoot phenomenon and simulating the thermal-controlled phase change. For the BNL test case run 309 as an example, Figure 2 compares the prediction of axial void fraction and pressure profile using different models with the experimental data. The void fraction provided by Le et al. [41] conforms well with the measurement, while the pressure profile of Liao and Lucas [40] gives the best agreement. In comparison to axial profiles, prediction of the lateral distribution of void fraction is even more challenging.

3.2. Pipe blowdown

Jo et al. [159, 160] investigated water flashing flow from a PWR steam generator (SG) by a feed water line break (FWLB) accident using the commercial CFD code ANSYS CFX. The simplified SG model and broken position is sketched in Figure 3(a). The space occupied by the tube bundle in the SG secondary side was simulated with the porous medium model. The discharge flow accompanying with thermal phase change was calculated by employing the NHNEM two-fluid model, governing equations were solved for the liquid and vapor phases separately. The gas phase consisted of discrete spherical bubbles with a uniform size. The $k-\omega$ SST model was used to estimate the turbulent viscosity. The phase change was driven by temperature difference and interphase heat transfer. Transient pressure, velocity, void fraction response of the SG secondary side and the broken pipe side was analyzed. Vapor was built firstly at the exit of the broken pipe, and developed along the pipe wall with a liquid core towards SG. The FWLB accident resulted in steep escalation of the SG secondary flow velocities, especially near the broken pipe. Figure 3(b) plots the mixture velocity responses at four monitoring points for the first 0.3 s, where the distance to the broken position decreases from point 1 to point 4. At the exit of the broken nozzle (point 4), the velocity is over 100 m/s, which may cause mechanical damage on some tubes. The authors investigated the effect of initial state of the fluid upstream the broken pipe end, i.e. subcooled water, saturated steam or saturated water-steam mixture. It was found that the subcooled water non-flashing flow model gives the maximum discharge flow rate, the saturated water flashing flow model the minimum, while the sub-cooled water flashing flow model ranges between. In addition, the simulation results were shown to have a sensitive dependence on the initial interfacial area density related to the choice of gas volume fraction and bubble mean diameter.

Karathanassis et al. [156] presented CFD simulations of flashing flow from the Edwards pipe blowdown [42] in addition to two discharge nozzles. A sketch of the pipe as well as the measurement points (P1 $\sim$ P7) is depicted in Figure 4. As aforementioned their numerical studies were based on the two-phase

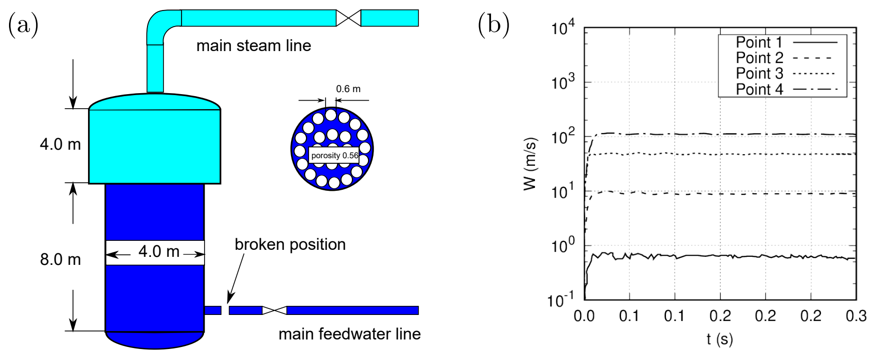

Figure 3: CFD simulation of FWLB induced discharge flow from SG [160]. (a) Simplified SG model (b) Transient velocity response at different monitoring points: Point 1 (SG center at the broken pipe level), Point 2 (first upstream point of the broken pipe in SG), Point 3 (second upstream point of the broken pipe in SG), Point 4 (center of the cross-section at the mid point of the broken pipe)

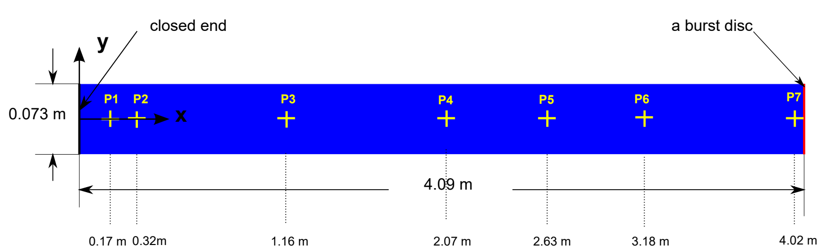

Figure 4: Sketch of the Edwards blowdown experiments [42]

mixture model assuming zero slip velocity. They evaluated the capability of various mass-transfer rate models. The interfacial area density A_i was calculated assuming a nucleation site density of 10^{13} m^{-3} and a bubble radius of 10^{-6} m. In other words, A_i remains constant during the phase change process, which deviates obviously from the physical picture. For the blowdown case, three formulations of the PPCM model based on the H-K equation, i.e. HK1, HK2, HK3, were compared with the HRM model. The HK2 model computes the interfacial mass flux in a way similar to Eq. 12, while in HK1 it is simplified as

$$\dot{\Gamma} = A_i C_{evap} \alpha_l \rho_l \left(0.195\rho k + p_{sat} - p\right), \tag{18}$$

where C_{evap} is an empirical coefficient (= 0.001 in the investigation case). In the HK3 formulation the temperature discontinuity at the interface was considered, i.e.

$$\dot{\Gamma} = \frac{A_i \beta}{\sqrt{2\pi R T_{sat}}} \left(\frac{0.195\rho k + p_{sat}}{\sqrt{T_l}} - \frac{p}{\sqrt{T_{sat}}} \right). \tag{19}$$

The value of 0.1 was used for the accommodation coefficient β.

Figures 5 (a) and (b) display the comparison of the numerical predictions of transient pressure and void fraction to experimental data. One can see that all the models have difficulty in capturing the flashing-inception, but the PPCM model based on the H-K equation gives overall better results compared to the HRM model.

Liao and Lucas [1] investigated the same case with the TPCM model in ANSYS CFX. Apart from the different phase change model, they accounted for the interphase slip velocity using the two-fluid model. A constant value of 1.0 mm was assumed for the bubble diameter, but the interfacial area density was allowed to increase with the bubble number density as a result of phase change. The comparison of the simulation results with those from [156] and experimental data is shown in Figure 6. As expected, a better agreement was achieved by using the TPCM model at the early stage of blowdown. The pressure undershoot at the very beginning was captured well, which evidences the importance of

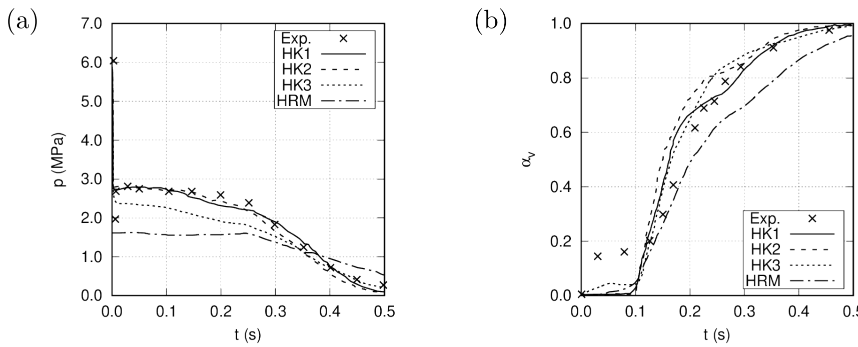

Figure 5: Edwards pipe simulation results from [156]: (a) pressure at P7 (b) void fraction at P4

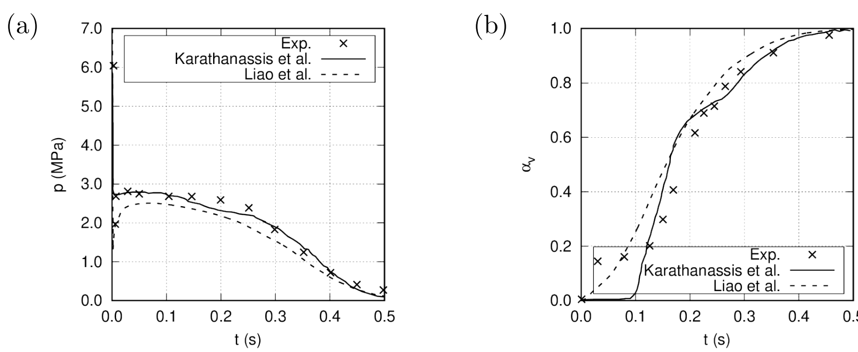

Figure 6: Edwards pipe simulation results from [1]: (a) pressure at P7 (b) void fraction at P4

thermal non-equilibrium at this stage.

3.3. Flashing-induced instability (FII)

As discussed in the previous section, the FII problem concerning nuclear safety analysis has been investigated intensively with experiments and system codes, whereas CFD simulations are scarce. The challenges comprise high-amplitude high-frequency waves, large geometry sizes and lack of CFD-grade experimental data. Liao et al. [1, 161, 162] presented CFD studies on the flashing and FII phenomenon observed at two test facilities, i.e. the AREVA INKA test facility [69] and the TUD GENEVA facility [78]. Both of them are down-

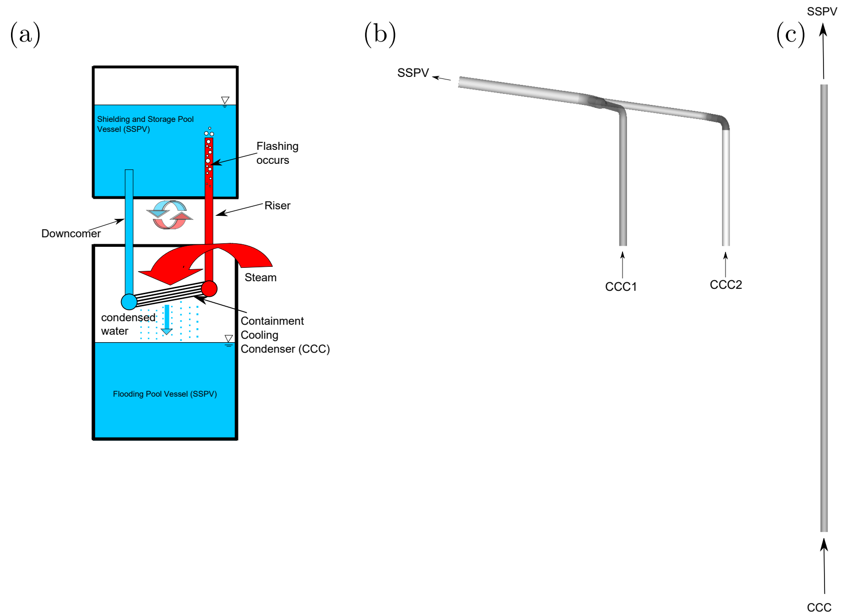

Figure 7: (a) KERENA$^{\text{TM}}$ CCC system, (b) INKA riser [69, 161], (c) GENEVA riser [78, 162]

scale models of the containment cooling condenser (CCC) of the KERENA$^{\text{TM}}$ reactor, whose function and principle is sketched in Figure 7 (a). In case of containment overpressure, steam condensed on the surface of the CCC tubes and the heat is transported by the cooling water inside the tubes via the riser to SSPV. In the INKA test facility, two sets of CCC were constructed and the riser connecting CCC1 and CCC2 with SSPV comprises of vertical and sloped pipes, see Figure 7 (b), while the GENEVA riser is a single straight pipe, which is much longer as shown in Figure 7 (c).

Both simulations [1, 162] were performed with the two-fluid model in ANSYS CFX, and the computational domain was restricted to the riser for high efficiency. The liquid and vapor phases were assumed in pressure equilibrium, and the TPCM was activated for interphase mass transfer. Bubbles have a spherical shape and the number density was prescribed as a constant value ($N_b = 5\times10^4$). Single-phase inlet was assumed, and the boundary conditions such as inlet mass flow rate, liquid temperature and outlet pressure were defined according to the

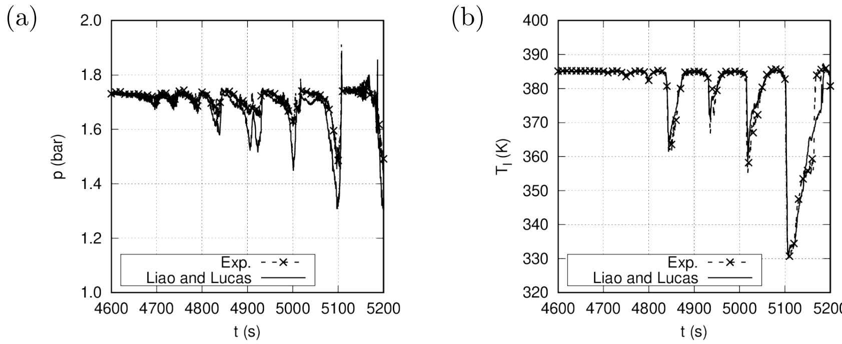

Figure 8: Comparison between simulation and measurement of pressure and temperature fluctuation in the INKA riser [1] (a) Pressure at CCC1, (b) Temperature at outlet

measurements. Figure 8 presents cross-section averaged pressure and temperature transients inside the INKA riser, which conform well to the experimental results. The simulation showed that the onset of flashing occurs at the highest point of the domain due to low hydrostatic pressure, i.e. the top wall at the outlet, and then propagated downward to the inlets. Separated and dispersed flow was developed in the sloped and vertical pipe, respectively, and instability waves were observed at the interface, see Figure 9. As the pressure recovered the steam disappeared from bottom to top of the domain.

In order to reflect the non-uniform distribution of vapor bubbles at the cross section of the pipe, needle-shaped conductivity probes were installed in the central and the peripheral region (about 2/3 of the inner diameter) at the GENEVA test facility. Liao et al. [162] compared the local void fraction obtained numerically and experimentally, which discovered substantial difference. As shown in Figure 10 the onset of flashing was delayed in the simulation. For example, according to the experiment at z=3.99 m bubbles appear at the pipe center before t = 20 s. On the other hand, the simulation gives non-zero void fraction after t = 50 s. Furthermore, the void fraction in the near-wall region is under-predicted, see Figure 10 (b) and 10 (d). This discrepancy is partly caused by the inaccurate prediction of bubble size, since non-drag forces representing the lateral movement of bubbles depend on it directly. The assumption of a

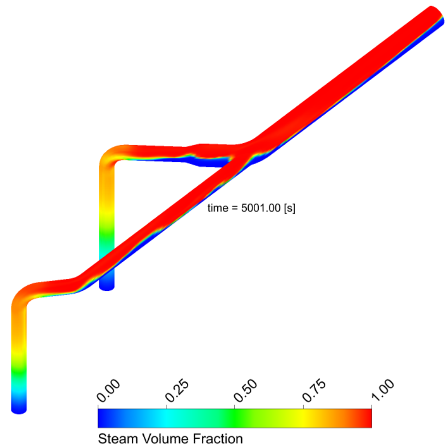

Figure 9: Steam distribution in the INKA riser [161]

constant bubble number density deviates from the reality, leading to a uniform local bubble size, which is either smaller or larger than the real mean value. In this case, it might be over-predicted, since the bubbles are accumulated in the pipe center due to the effect of lift force. Nevertheless, both simulation and experiment evidenced that the flashing was initiated earlier at the pipe center than the periphery. Good agreement on the central void fraction was achieved at z = 4.99 m (see Figure 10 (c)).

3.4. Pressure relief transient

As shown in previous examples, flashing flows represent heterogeneous mixture of liquid and gas with void fraction ranging from zero to one. Reliable prediction of local phase distribution with the CFD tool represents still a challenge relative to the cross-section averaged parameters such as pressure and temperature. To improve the simulation results, it is of prime importance to reproduce the bubble size change appropriately with the model, although equivalent efforts are needed in modelling of bubble forces, interphase heat transfer as well as two-phase turbulence. For the purpose of model development, high-resolution high-quality experimental data are valuable. Lucas et al. [163] presented experiments on flash evaporation in an 8 m long vertical pipe with an inner diameter

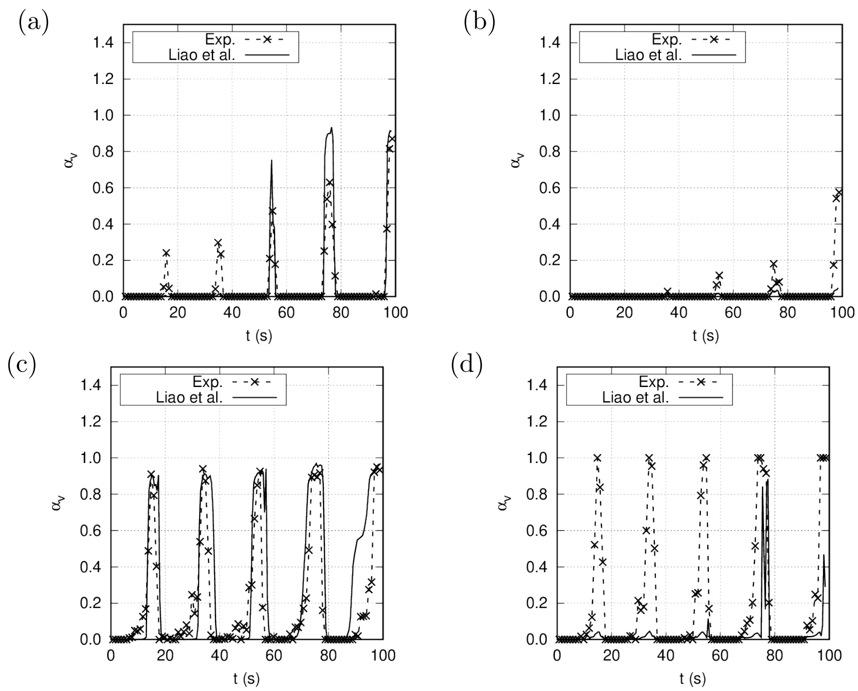

Figure 10: Comparison between simulation and measurement of local vapor void fraction inside the riser [162] (a) pipe center, z=3.99 m (b) 2/3 of the inner diameter, z=3.99 m (c) pipe center, z=4.99 m (d) 2/3 of the inner diameter, z=4.99 m

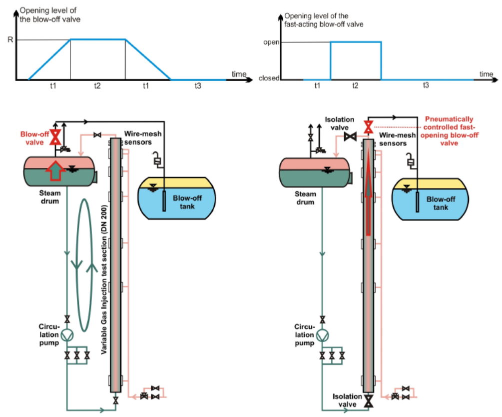

(a) procedure 1 (b) procedure 2

Figure 11: Pressure relief experiments at the TOPFLOW facility [163]

of 195.3 mm, carried out at the TOPFLOW facility. The phase change was induced by depressurization of the pipe from 1, 2, 4 and 6.5 MPa. The pressure relief transient and evaporation process was investigated for circulating and stagnant water, respectively, each with a different blow-off valve opening/closing procedure, see Figure 11. Detailed information on the structure of gas-liquid interfaces including spatial and temporal void fraction, bubble size distribution as well as gas velocities was obtained by using a pair of wire-mesh sensors. Measurements are available for different combinations of opening/closing speed and maximum opening degrees of the valve, which are represented by the parameters R, t1, t2 and t3 in Figure 11. The database is suitable for the development and validation of CFD models. Liao et al. [147, 164] presented detailed CFD studies on the TOPFLOW pressure relief test cases based on the two-fluid model with thermal phase change. The main focus was put on evaluating methods for estimation of bubble diameter and interfacial area density, which vary from assuming a constant bubble diameter or number density to using a poly-dispersed approach. The main findings are summarized as follows:

- Mono-disperse approaches fail in predicting the bubble size change and thus the lateral movement of bubbles.

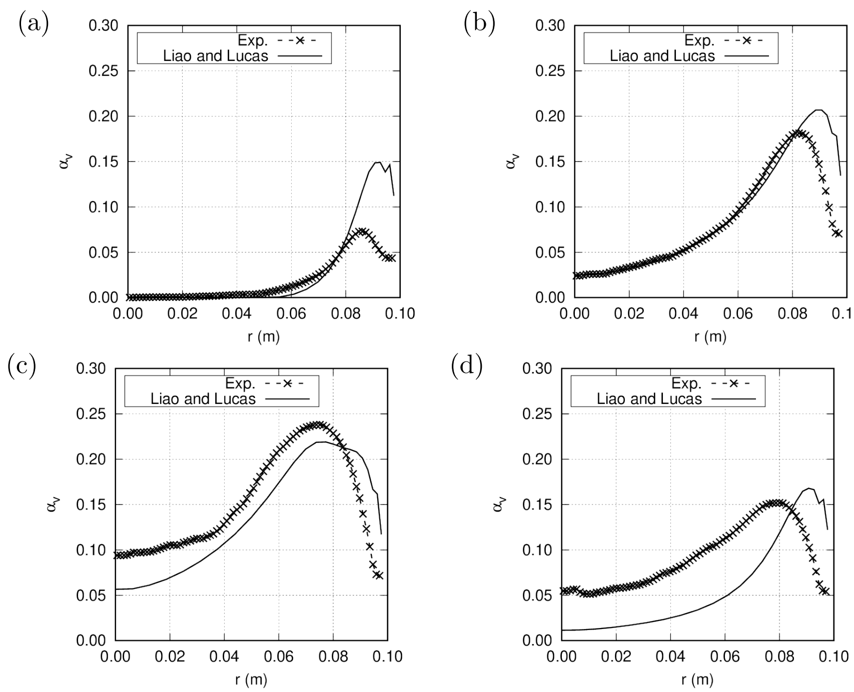

Figure 12: Comparison between simulated and measured radial void fraction profile at (a) t = 37 s, (b) t = 49 s, (c) t = 55 s, (d) t = 67 s

- The prescribed value for bubble diameter or number density affects the onset of flashing as well the evaporation rate in the simulation. A too large bubble diameter fails to trigger the phase change, while a too small one initiates it too early.

- The contribution of wall and bulk nucleation decreases and increases respectively with the pressure level.

- The poly-disperse approach with appropriate closures for bubble nucleation, coalescence and breakup improves the simulation results considerably. Radial void fraction and bubble size distribution are well captured as shown in Figures 12 and 13.

Above CFD simulations of flashing flows are summarized in Table 3. They mainly differ in whether the velocity difference between phases is considered or

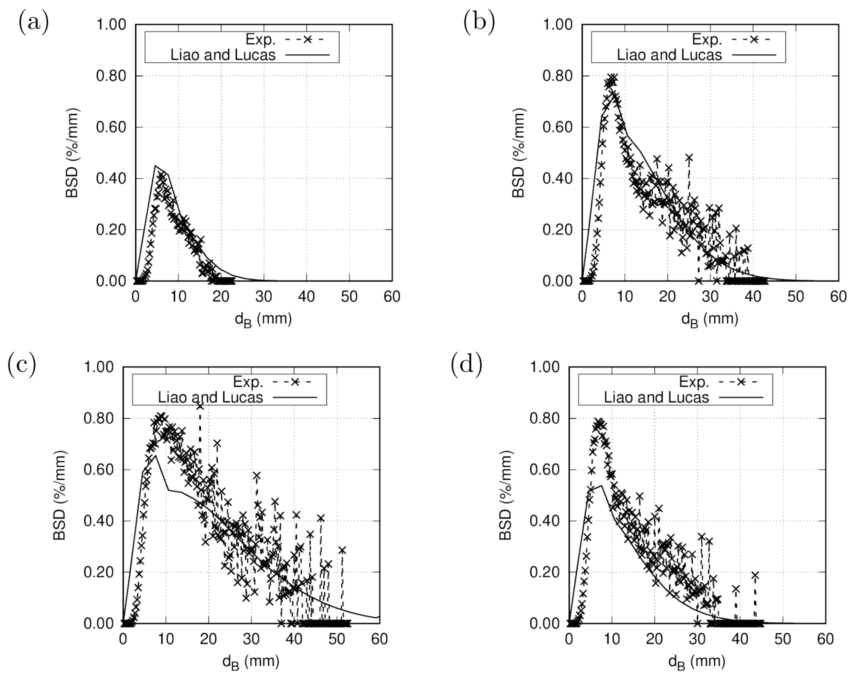

Figure 13: Comparison between simulated and measured radial void fraction profile at (a) t = 37 s, (b) t = 49 s, (c) t = 55 s, (d) t = 67 s

not (mixture or two-fluid model), what kind of phase change models (TPCM, PPCM, HRM or HEM) are adopted, and how to determine the interfacial area density (constant N_B, d_B, variable N_B or poly-dispersity).

References and code	Numerical models and assumptions	Experiment
[35] ANSYS CFX 4.2	• homogeneous mixture model • TPCM • vapor at saturation • transport equation for N_B • wall nucleation considered	BNL nozzle [26]
[37] ANSYS FLUENT	• two-fluid model • non-drag forces neglected • TPCM • interface at saturation • heat transfer on vapor side neglected • transport equation for N_B • wall nucleation considered	BNL nozzle [26]
[39] ANSYS CFX 15.0	• two-fluid model • drag and non-drag forces considered • TPCM • vapor and interface at saturation • transport equation for N_B • wall and bulk nucleation considered	BNL nozzle [26]
[40] ANSYS CFX 15.0	• two-fluid model • drag and non-drag forces considered • TPCM • vapor and interface at saturation • prescribed value N_B	BNL nozzle [26]
[145] NEPTUNE_CFD	• two-fluid model • drag and added mass force considered • TPCM	Moby Dick nozzle [146]

	• vapor and interface at saturation • prescribed value für d_B • wall nucleation considered as a mass source	
[36] ANSYS FLUENT 6.1	• homogeneous mixture model • PPCM based on the R-P equation	BNL nozzle [26]
[150] ANSYS FLUENT 12.0.16	• homogeneous mixture model • PPCM based on the R-P equation	Moby Dick nozzle [146] LSTF SGTR [151]
[38]	• homogeneous mixture model • PPCM based on the H-K equation	BNL nozzle [26]
[41]	• homogeneous mixture model • slip model • PPCM based on the H-K equation	BNL nozzle [26]
[139] in-house code	• homogeneous mixture model • TPCM model • PPCM based on the H-K equation	BNL nozzle [26]
[3] OpenFOAM	• homogeneous mixture model • relaxation model (HRM)	pipe flow [153, 154]
[155] NEPTUNE_CFD	• two-fluid model • very large drag forces • DEM model	Moby Dick nozzle [146]
[159, 160] ANSYS CFX	• two-fluid model • non-drag neglected • TPCM model • prescribed value for d_B	SG FWLB accident
[156] ANSYS FLUENT	• homogeneous mixture model • PPCM based on the R-P equation • PPCM based on the H-K equation • compared with the HEM, HRM model	Moby Dick nozzle [146] ”Reitz” nozzle [157] ”Edwards” pipe [42]
[1] ANSYS CFX 15.0	• two-fluid model • TPCM	”Edwards” pipe [42] INKA FII [69]

	• drag and non-drag cosidered • prescribed value for d_B or N_B	
[162] ANSYS CFX 18.0	• two-fluid model • TPCM • drag and non-drag cosidered • prescribed value for N_B	GENEVA FII [78]
[162] ANSYS CFX 18.2	• two-fluid model • TPCM • drag and non-drag cosidered • population balance model • wall and bulk nucleation considered • coalescence and breakup considered	TOPFLOW [163]

Table 3: Summary of CFD studies on flashing flows

4. Conclusion

Although the numerical methods and models that have been used for analysis of flashing phenomena differ largely, there is some consensus concerning following points:

- In most cases, it is necessary to account for interfacial slip appropriately by using the two-fluid model.

- Non-equilibrium phase change model is more general than the relaxation and equilibrium model. Thermal phase change model is superior to pressure phase change model, when thermal non-equilibrium effects are significant.

- Convection has a considerable contribution to the interfacial heat transfer in flashing flow, and conduction is dominant only in a short time after nucleation.

- Appropriate modelling of bubble size and interfacial area density is crucial in modelling the interphase transfer. Taking into account the polydispersity is recommended by several researchers.

- It is difficult to reproduce the lateral motion of bubbles, where non-drag forces play an important role in the interphase momementum transfer.

The prime challenges in CFD simulation of flashing flows arise from choosing appropriate closure models for interphase transfer, bubble dynamics (nucleation, coalescence and breakup) as well two-phase turbulence. Further efforts regarding model improvement and data acquisition are required. Although temperature difference is deemed to be the predominant driving force for phase change in flashing situations, the effect of pressure difference might be substantial at the inception, in particular at a large pressure undershoot. In most of the simulations, either pressure difference or temperature difference was neglected. There is insufficient discussion on how to combine the two driving forces for phase change properly. At high void fractions, the flow regime deviates widely from bubbly flow, whereas the assumption of spherical bubbles were made in the majority of works. Extending a multi-scale multi-field approach, for example the GENTOP model proposed by Hänsch et al. [165], to handle different bubble shapes is of interest in the future. Höhne et al. [166] and Höhne and Lucas [167] have demonstrated the application of this model for various boiling cases.

Declarations of interest: none.

References

[1] Y. Liao, D. Lucas, Possibilities and limitations of CFD simulation for flashing flow scenarios in nuclear applications, Energies 10 (1) (2017) 139:1–22.

[2] Y. Liao, D. Lucas, Computational modelling of flash boiling flows: A literature survey, International Journal of Heat and Mass Transfer 111 (2017) 246–265.

[3] D. P. Schmidt, S. Gopalakrishnan, H. Jasak, Multi-dimensional simulation of thermal non-equilibrium channel flow, International Journal of Multiphase Flow 36 (4) (2010) 284–292.

[4] M. Alamgir, J. Lienhard, Correlation of pressure undershoot during hot-water depressurization, Journal of Heat Transfer 103 (1981) 52–55.

[5] M. Maria Antony Raj, K. Kalidasa Murugavel, T. Rajaseenivasan, K. Srithar, A review on flash evaporation desalination, Desalination and Water Treatment 57 (29) (2016) 13462–13471.

[6] Q. Yang, B. Zhao, D. Zhang, Y. Wang, J. Yan, Experimental study on heat transfer characteristics in static flash evaporation of aqueous nacl solution, International Journal of Heat and Mass Transfer 102 (2016) 1093–1099.

[7] J. Stengler, K. Schaber, S. Mall-Gleissle, Experimental study on low temperature desalination by flash evaporation in a novel compact chamber design, Desalination 448 (2018) 103–112.

[8] Q. Chen, Y. Li, K. Chua, et al., Experimental and mathematical study of the spray flash evaporation phenomena, Applied Thermal Engineering 130 (2018) 598–610.

[9] E. Sher, T. Bar-Kohany, A. Rashkovan, Flash-boiling atomization, Progress in energy and combustion science 34 (4) (2008) 417–439.

[10] M. Levy, E. Sher, Transition from heterogeneous to homogeneous nucleation in a simple structure flash-boiling atomizer, Atomization and Sprays 20 (10) 905–907.

[11] D. Ju, C. Wang, X. Qiao, J. Xiao, Z. Huang, Internal flow pattern and macroscopic characteristics of a flash-boiling spray actuated through a twin-orifice atomizer with low injection pressure, Atomization and Sprays 26 (4) (2016) 377–410.

[12] T. Alghamdi, S. T. Thoroddsen, J. Hernández-Sánchez, Ultra-high speed visualization of a flash-boiling jet in a low-pressure environment, International Journal of Multiphase Flow 110 (2019) 238–255.

[13] A. Mansour, N. Müller, A review of flash evaporation phenomena and resulting shock waves, Experimental Thermal and Fluid Science 107 (2019) 146–168.

[14] G. Lamanna, H. Kamoun, B. Weigand, J. Steelant, Towards a unified treatment of fully flashing sprays, International Journal of Multiphase Flow 58 (2014) 168–184.

[15] M. El Haj Assad, E. Bani-Hani, M. Khalil, Performance of geothermal power plants (single, dual, and binary) to compensate for LHC-CERN power consumption: comparative study, Geothermal Energy 5 (1) (2017) 17:1–16.

[16] S. Zheng, X. Xie, Y. Jiang, Experimental study on the flash evaporation process of LiBrH2O solution in an absorption heat pump, International Journal of Refrigeration 61 (2016) 117–126.

[17] C. Danţuş, G. Rusu, M. Dobromir, M. Rusu, Preparation and characterization of CdO thin films obtained by thermal oxidation of evaporated cd thin films, Applied Surface Science 255 (5) (2008) 2665–2670.

[18] S. Mutair, Y. Ikegami, Study and enhancement of flash evaporation desalination utilizing the ocean thermo cline and discharged heat, International Journal of Electrical and Computer Engineering 2 (7) (2008) 1385–1392.

[19] A. Muthunayagam, K. Ramamurthi, J. Paden, Low temperature flash vaporization for desalination, Desalination 180 (1-3) (2005) 25–32.

[20] Y. Zhang, J. Wang, J. Yan, D. Chong, J. Liu, Experimental study on energy transformation and separation characteristic of circulatory flash evaporation, International Journal of Heat and Mass Transfer 99 (2016) 862–871.

[21] G. Wallis, Critical two-phase flow, International Journal of Multiphase Flow 6 (1-2) (1980) 97–112.

[22] G. A. Pinhasi, A. Ullmann, A. Dayan, Modeling of flashing two-phase flow, Reviews in Chemical Engineering 21 (3-4) (2005) 133–264.

[23] M. Reocreux, Contribution to the study of critical flow rates in two-phase water vapor flow, Vol. 3, US Nuclear Regulatory Commission, 1977.

[24] V. Schrock, E. Starkman, R. Brown, Flashing flow of initially subcooled water in convergent–divergent nozzles, Journal of Heat Transfer 99 (2) (1977) 263–268.

[25] E. Studsvik, Marviken full-scale critical-flow tests. volume 22. results from test 14. final report, Tech. rep., Studsvik Energiteknik AB (1982).

[26] N. Abuaf, B. Wu, G. Zimmer, P. Saha, Study of nonequilibrium flashing of water in a converging-diverging nozzle. volume 1: experimental, Tech. rep., Brookhaven National Lab., Upton, NY (USA) (1981).

[27] F. Moody, Maximum flow rate of a single component, two-phase mixture, Journal of Heat Transfer 87 (1) (1965) 134–141.

[28] R. Henry, H. Fauske, The two-phase critical flow of one-component mixtures in nozzles, orifices, and short tubes, Journal of Heat Transfer 93 (2) (1971) 179–187.

[29] H. Richter, Separated two-phase flow model: Application to critical two-phase flow, International Journal of Multiphase Flow 9 (5) (1983) 511–530.

[30] P. Saha, N. Abuaf, B. Wu, A nonequilibrium vapor generation model for flashing flows, Journal of Heat Transfer 106 (1984) 198–203.

[31] B. Wu, N. Abuaf, P. Saha, Study of nonequilibrium flashing of water in a converging-diverging nozzle. volume 2. modeling, Tech. rep., Brookhaven National Lab., Upton, NY (USA) (1981).

[32] J. Riznic, M. Ishii, N. Afgan, Mechanistic model for void distribution in flashing flow, Tech. Rep. No. CONF-8705224–1, Institut za Nuklearne Nauke Boris Kidric (1987).

[33] I. Tiselj, S. Petelin, Modelling of the critical flashing flow in the nozzle with RELAP5 equations, in: Annual Meeting of the Nuclear Society of Slovenia, 1994.

[34] J. Muñoz-Cobo, E. Cerezo, S. Chiva, Two phase flow modelling of flashing critical and non critical flows in converging-diverging nozzles, in: The 4th International Conference on Multiphase Flow, ICMF-4, 2001.

[35] S. Maksic, D. Mewes, CFD-calculation of the flashing flow in pipes and nozzles, in: ASME 2002 Joint US-European Fluids Engineering Division Conference, 2002.

[36] G. Palau-Salvador, P. González-Altozano, J. Arviza-Valverde, Numerical modeling of cavitating flows for simple geometries using fluent V6. 1, Spanish Journal of Agricultural Research 5 (4) (2007) 460–469.

[37] C. Marsh, A. O'Mahony, Three-dimensional modelling of industrial flashing flows, Progress in Computational Fluid Dynamics, an International Journal 9 (6-7) (2009) 393–398.

[38] D.-M. Liu, S.-H. Liu, Y.-L. Wu, H.-Y. Xu, A thermodynamic cavitation model applicable to high temperature flow, Thermal Science 15 (suppl. 1) (2011) 95–101.

[39] J. P. Janet, Y. Liao, D. Lucas, Heterogeneous nucleation in CFD simulation of flashing flows in converging–diverging nozzles, International Journal of Multiphase Flow 74 (2015) 106–117.

[40] Y. Liao, D. Lucas, 3D CFD simulation of flashing flows in a converging-diverging nozzle, Nuclear Engineering and Design 292 (2015) 149–163.

[41] D. Q. Le, R. Mereu, G. Besagni, V. Dossena, F. Inzoli, Computational fluid dynamics modeling of flashing flow in convergent-divergent nozzle, Journal of Fluids Engineering 140 (10) 101102:1–22), year=2018, publisher=American Society of Mechanical Engineers Digital Collection.

[42] A. Edwards, T. O'brien, Studies of phenomena connected with the depressurization of water reactors, J. Brit. Nucl. Energy Soc 9 (2) (1970) 125–135.

[43] K. Wolfert, The simulation of blowdown processes with condensation of thermodynamic nonequilibrium phenomena, in: OECD/NEA Specialists Mtg on Transient Two-Phase Flow, 1976.

[44] K. Carlson, V. Ransom, R. Wagner, Application of relap5 to a pipe blowdown experiment, Tech. rep., Idaho National Engineering Lab. (1980).

[45] G. Pinhasi, Source term modeling of gas and liquid releases from a breached pressure vessel, Ph.D. thesis, Tel-Aviv University (2001).

[46] Y. Takeda, S. Toda, Pressure oscillation in subcooled decompression under temperature gradient, Journal of Nuclear Science and Technology 16 (7) (1979) 484–495.

[47] N. Lafferty, V. Ransom, M. Lopez-de Bertodano, Relap5 analysis of two-phase decompression and rarefaction wave propagation under a temperature gradient, Nuclear Technology 169 (1) (2010) 34–49.

[48] O. Costa, I. Tiselj, L. Cizelj, Depressurization of vertical pipe with temperature gradient modeled with waha code, Science and Technology of Nuclear Installations 2012 951923:1–9), year=2012, publisher=Hindawi.

[49] J. Lienhard, M. Alamgir, M. Trela, Early response of hot water to sudden release from high pressure, Journal of Heat Transfer 100 (1978) 473–479.

[50] J. Bartak, A study of the rapid depressurization of hot water and the dynamics of vapour bubble generation in superheated water, International journal of multiphase flow 16 (5) (1990) 789–798.

[51] F. D'Auria, Thermal-Hydraulics of water cooled nuclear reactors, woodhead publishing, 2017.

[52] H. Fenech, Heat transfer and fluid flow in nuclear systems, Elsevier, 2013.

[53] G. Brockett, H. Curet, H. W. Heiselmann, Experimental investigations of reactor system blowdown., Tech. rep., Idaho Nuclear Corp., Idaho Falls (1970).

[54] B. Slifer, A. Rogers, Loss-of-coolant accident and emergency core cooling models for general electric boiling water reactors., Tech. rep., General Electric Co., San Jose, Calif. Atomic Power Equipment Dept. (1971).

[55] C. Crowley, Analysis of Flashing Transient Effects During Refill: Topical Report, Vol. 88, The Commission, 1981.

[56] G. Wang, Y. Yan, S. Shi, Z. Dang, X. Yang, M. Ishii, Experimental study of blowdown event in a pwr-type small modular reactor, Nuclear Technology 205 (1-2) (2019) 297–306.

[57] A. Ylönen, Large break blowdown test facility study, Master's thesis, Lappeenranta University of Technology (2008).

[58] S. Revankar, B. Wolf, A. Vadlamani, Assessment of leak rates through steam generator tubes, Tech. rep., Purdue University, West Lafayette, IN, Final Report to Canadian Nuclear Safety Commission, PU/NE-13-11 (2013).

[59] J. Zhang, H. Yu, M. Wang, Y. Wu, W. Tian, S. Qiu, G. Su, Experimental study on the flow and thermal characteristics of two-phase leakage through micro crack, Applied Thermal Engineering 156 (2019) 145–155.

[60] K. Tasaka, et al., ROSA-IV large scale test facility (LSTF) system description for second simulated fuel assembly, Tech. rep., Japan Atomic Energy Research Institute (1990).

[61] R. Dimenna, Semiscale steam-generator tube-rupture test results, Tech. rep., EG and G Idaho (1983).

[62] G. Loomis, Results of the semiscale Mod-2B steam generator tube rupture test series, Tech. rep., EG and G Idaho (1985).

[63] G. De Santi, Analysis of steam generator u-tube rupture and intentional depressurization in lobi-mod2 facility, Nuclear engineering and design 126 (1) (1991) 113–125.

[64] S. G. Lim, H. C. No, S. W. Lee, H. G. Kim, J. Cheon, J. M. Lee, S. M. Ohk, Development of stability maps for flashing-induced instability in a passive containment cooling system for ipower, Nuclear Engineering and Technology 52 (1) (2020) 37–50.

[65] T. Schulz, Westinghouse ap1000 advanced passive plant, Nuclear Engineering and Design 236 (14-16) (2006) 1547–1557.

[66] W. Zhou, B. Wolf, S. Revankar, Assessment of relap5/mod3. 3 condensation models for the tube bundle condensation in the pccs of esbwr, Nuclear Engineering and Design 264 (2013) 111–118.

[67] S. W. Lee, S. Heo, H. U. Ha, H. G. Kim, The concept of the innovative power reactor, Nuclear Engineering and Technology 49 (7) (2017) 1431–1441.

[68] A. Bakhmet'Ev, M. Bol'Shukhin, V. Vakhrushev, A. Khizbullin, O. Makarov, V. Bezlepkin, S. Semashko, I. Ivkov, Experimental validation of the cooling loop for a passive system for removing heat from the aes-2006 protective envelope design for the leningradskaya nuclear power plant site, Atomic energy 106 (3) (2009) 185–190.

[69] S. Leyer, M. Wich, The integral test facility karlstein, Science and Technology of Nuclear Installations 2012.

[70] J. Xing, D. Song, Y. Wu, HPR1000: Advanced pressurized water reactor with active and passive safety, Engineering 2 (1) (2016) 79–87.

[71] E. Wissler, H. Isbin, N. Amundson, Oscillatory behavior of a two-phase natural-circulation loop, AIChE Journal 2 (2) (1956) 157–162.

[72] A. Manera, T. van der Hagen, Stability of natural-circulation-cooled boiling water reactors during startup: experimental results, Nuclear technology 143 (1) (2003) 77–88.

[73] M. Furuya, F. Inada, T. van der Hagen, Flashing-induced density wave oscillations in a natural circulation bwr—mechanism of instability and stability map, Nuclear engineering and design 235 (15) (2005) 1557–1569.

[74] C. Marcel, M. Rohde, T. van der Hagen, Experimental and numerical investigations on flashing-induced instabilities in a single channel, Experimental thermal and fluid science 33 (8) (2009) 1197–1208.

[75] C. Marcel, M. Rohde, T. van der Hagen, Experimental investigations on flashing-induced instabilities in one and two-parallel channels: A comparative study, Experimental Thermal and Fluid Science 34 (7) (2010) 879–892.

[76] H. Khartabil, A flashing driven moderator cooling system for candu reactors: Experimental and computational results, Tech. rep. (2000).

[77] S.-K. Yang, Stability of flashing-driven natural circulation in a passive moderator cooling system for canadian scwr, Nuclear engineering and design 276 (2014) 259–276.

[78] T. Cloppenborg, C. Schuster, A. Hurtado, Two-phase flow phenomena along an adiabatic riser–an experimental study at the test-facility geneva, International Journal of Multiphase Flow 72 (2015) 112–132.

[79] J. Andersen, F. Inada, L. Klebanov, TRACG analyses of flashing instability during start-up, in: The 21st International Conference on Nuclear Engineering, ICONE-3, 1995.

[80] A. Manera, U. Rohde, H.-M. Prasser, T. van der Hagen, Modeling of flashing-induced instabilities in the start-up phase of natural-circulation bwrs using the two-phase flow code flocal, Nuclear Engineering and Design 235 (14) (2005) 1517–1535.

[81] Y. Kozmenkov, U. Rohde, A. Manera, Validation of the relap5 code for the modeling of flashing-induced instabilities under natural-circulation conditions using experimental data from the circus test facility, Nuclear engineering and design 243 (2012) 168–175.

[82] Q. Wang, P. Gao, X. Chen, Z. Wang, Y. Huang, An investigation on flashing-induced natural circulation instabilities based on relap5 code, Annals of Nuclear Energy 121 (2018) 210–222.

[83] J. Jeong, K. Ha, B. Chung, W. Lee, Development of a multi-dimensional thermal-hydraulic system code, mars 1.3. 1, Annals of Nuclear Energy 26 (18) (1999) 1611–1642.

[84] H. K. Fauske, Contribution to the theory of two-phase, one-component critical flow, Tech. rep., Argonne National Lab., Ill. (1962).

[85] H. Isbin, J. Moy, A. Da Cruz, Two-phase, steam-water critical flow, AIChE Journal 3 (3) (1957) 361–365.

[86] F. Zaloudek, The low pressure critical discharge of steam-water mixtures from pipes, Tech. rep., General Electric Co. Hanford Atomic Products Operation, Richland, Wash. (1961).

[87] D. W. Faletti, R. Moulton, Two-phase critical flow of steam-water mixtures, AIChE Journal 9 (2) (1963) 247–253.

[88] F. Inada, O. T., Thermo-hydraulic instability of natural circulation BWRs (explanation on instability mechanisms at start-up by homogeneous and thermo-dynamic equilibrium model considering flashing effect), in: International Conference on New Trends in Nuclear System Thermohydraulics, 1994.

[89] D. Van Bragt, W. De Kruijf, A. Manera, T. van der Hagen, H. van Dam, Analytical modeling of flashing-induced instabilities in a natural circulation cooled boiling water reactor, Nuclear engineering and design 215 (1-2) (2002) 87–98.

[90] S. Levy, Prediction of two-phase critical flow rate, Journal of Heat Transfer 87 (1) (1965) 53–57.

[91] R. Hu, M. Kazimi, Flashing-induced instability analysis and the start-up of natural circulation boiling water reactors, Nuclear technology 176 (1) (2011) 57–71.

[92] F. Inada, M. Furuya, A. Yasuo, Thermo-hydraulic instability of boiling natural circulation loop induced by flashing (analytical consideration), Nuclear Engineering and Design 200 (1-2) (2000) 187–199.

[93] A. Attou, M. Giot, J.-M. Seynhaeve, Modelling of steady-state two-phase bubbly flow through a sudden enlargement, International journal of heat and mass transfer 40 (14) (1997) 3375–3385.

[94] J. Bouré, Critical flow phenomenon with reference to two-phase flow and nuclear reactor systems, in: Thermal and hydraulic aspects of nuclear reactor safety. Vol. I, 1977.

[95] H. C. Simpson, R. Silver, Theory of one-dimensional, two-phase homogeneous non-equilibrium flow, in: Institute of Mechanical Engineers Symposium on Two-phase Fluid Flow, 1962.

[96] C. Lackme, Thermodynamics of critical two-phase discharge from long pipes of initially subcooled water, in: ICHMT Digital Library Online, Begel House Inc., 1982.

[97] S. Lee, V. Schrock, Critical two-phase flow in pipes for subcooled stagnation states with a cavity flooding incipient flashing model, Journal of Heat Transfer 112 (4) (1990) 1032–1040.

[98] E. Elias, P. Chambre, Flashing inception in water during rapid decompression, Journal of Heat Transfer 115 (1) (1993) 231–238.

[99] S. Levy, D. Abdollahian, Homogeneous non-equilibrium critical flow model, International Journal of Heat and Mass Transfer 25 (6) (1982) 759–770.

[100] J. J. Schröder, N. Vuxuan, Homogeneous non-equilibrium two-phase critical flow model, Chemical Engineering & Technology 10 (1) (1987) 420–426.

[101] E. Bauer, G. Houdayer, H. Sureau, A non-equilibrium axial flow model in application to loss-of-accident analysis. the cystere system code, in: OECD/NEA Specialists Meeting on Transient Two-phase flow, Atomic Energy of Canada, 1976.

[102] P. Kroeger, Application of a non-equilibrium drift flux model to two-phase blowdown experiments, Tech. rep., Brookhaven National Lab., Upton, NY (USA) (1976).

[103] Z. Bilicki, J. Kestin, Physical aspects of the relaxation model in two-phase flow, Proceedings of the Royal Society of London. A. Mathematical and Physical Sciences 428 (1875) (1990) 379–397.

[104] K. Neroorkar, S. Gopalakrishnan, R. Grover Jr, D. Schmidt, Simulation of flash boiling in pressure swirl injectors, Atomization and Sprays 21 (2) (2011) 179–188.

[105] E. T. Baldwin, R. O. Grover Jr, S. E. Parrish, D. J. Duke, K. E. Matusik, C. F. Powell, A. L. Kastengren, D. P. Schmidt, String flash-boiling in gasoline direct injection simulations with transient needle motion, International Journal of Multiphase Flow 87 (2016) 90–101.

[106] K. Saha, S. Som, M. Battistoni, Investigation of homogeneous relaxation model parameters and their implications for gasoline injectors, Atomization and Sprays 27 (4) (2017) 345–365.

[107] H. Guo, Y. Li, B. Wang, H. Zhang, H. Xu, Numerical investigation on flashing jet behaviors of single-hole gdi injector, International Journal of Heat and Mass Transfer 130 (2019) 50–59.

[108] C. Lackme, Incompleteness of the flashing of a supersaturated liquid and sonic ejection of the produced phases, International Journal of Multiphase Flow 5 (2) (1979) 131–141.

[109] M. De Lorenzo, P. Lafon, J.-M. Seynhaeve, Y. Bartosiewicz, Benchmark of delayed equilibrium model (dem) and classic two-phase critical flow models against experimental data, International Journal of Multiphase Flow 92 (2017) 112–130.

[110] U. Rohatgi, E. Reshotko, Non-equilibrium one-dimensional two-phase flow in variable area channels, in: Non-equilibrium two-phase flows; Proceedings of the Winter Annual Meeting, 1975.

[111] V. Blinkov, O. Jones, B. Nigmatulin, Nucleation and flashing in nozzles—2. comparison with experiments using a five-equation model for vapor void development, International Journal of Multiphase Flow 19 (6) (1993) 965–986.

[112] P. Deligiannis, J. Cleaver, The role of nucleation in the initial phases of a rapid depressurization of a subcooled liquid, International Journal of Multiphase Flow 16 (6) (1990) 975–984.

[113] E. Elias, S. Levy, P. Chambré, A mechanistic non-equilibrium model for two-phase critical flow, International Journal of Multiphase Flow 10 (1) (1984) 21–40.

[114] H. Atajafari, M. Nematollahi, M. Hashemi-Tilehnoee, N. Rafiee, et al., Validation of RELAP5/MOD3. 2 code for flashing-induced instabilities in a single channel, World Journal of Nuclear Science and Technology 5 (1) (2015) 6–17.

[115] M. Wein, Numerische simulation von kritischen und nahkritischen zweiphasenströmungen mit thermischen und fluiddynamischen nichtgleichgewichtseffekten, Ph.D. thesis, Technical University of Dresden (2002).

[116] J. Leung, A generalized correlation for one-component homogeneous equilibrium flashing choked flow, AIChE Journal 32 (10) (1986) 1743–1746.

[117] R. Hu, J. Zhao, S.-P. Kao, M. Kazimi, Thermal-hydraulic stability analysis of natural circulation bwrs, in: International Congress on Advances in Nuclear Power Plants (ICAPP 2007), 2007.

[118] M. Podowski, Modeling and analysis of two-phase flow instabilities, in: The 14th International Topical Meeting on Nuclear Reactor Thermalhydraulics, NURETH-10, 2003.

[119] P. Downar-Zapolski, Z. Bilicki, L. Bolle, J. Franco, The non-equilibrium relaxation model for one-dimensional flashing liquid flow, International journal of multiphase flow 22 (3) (1996) 473–483.

[120] H. Kato, H. Kayano, Y. Kageyama, A consideration of thermal effect on cavitation bubble growth, Tech. rep., American Society of Mechanical Engineers, New York, NY (United States) (1994).

[121] D. P. Schmidt, Cavitation in diesel fuel injector nozzles, Ph.D. thesis, University of Wisconsin–Madison (1997).

[122] S. Yin, N. Wang, H. Wang, Nucleation and flashing inception in flashing flows: A review and model comparison, International Journal of Heat and Mass Transfer 146 (2020) 118898.

[123] Z. Bilicki, R. Kwidziński, S. A. Mohammadein, Evaluation of the relaxation time of heat and mass exchange in the liquid-vapour bubble flow, International Journal of Heat and Mass Transfer 39 (4) (1996) 753–759.

[124] S. Mohammadein, The derivation of thermal relaxation time between two-phase bubbly flow, Heat and Mass Transfer 42 (5) (2006) 364–369.

[125] F. Dobran, Nonequilibrium modeling of two-phase critical flows in tubes, Journal of Heat Transfer 109 (1987) 731–738.

[126] M. S. Plesset, S. A. Zwick, The growth of vapor bubbles in superheated liquids, Journal of Applied Physics 25 (4) (1954) 493–500.

[127] E. Ruckenstein, On heat transfer between vapour bubbles in motion and the boiling liquid from which they are generated, Chemical Engineering Science 10 (1-2) (1959) 22–30.

[128] N. Zuber, J. Findlay, Average volumetric concentration in two-phase flow systems, Journal of Heat Transfer 87 (4) (1965) 453–468.

[129] H. Forster, N. Zuber, Growth of a vapor bubble in a superheated liquid, Journal of Applied Physics 25 (4) (1954) 474–478.

[130] Y. Liao, D. Lucas, Evaluation of interfacial heat transfer models for flashing flow with two-fluid cfd, Fluids 3 (2) (2018) 38.

[131] O. Jones Jr, N. Zuber, Bubble growth in variable pressure fields, Journal of Heat Transfer 100 (1978) 453–459.

[132] K. Ardron, A two-fluid model for critical vapour-liquid flow, International Journal of Multiphase Flow 4 (3) (1978) 323–337.

[133] W. Rivard, J. Travis, A nonequilibrium vapor production model for critical flow, Nuclear Science and Engineering 74 (1) (1980) 40–48.

[134] W. Ranz, W. Marshall, Evaporation from drops: Ii. chem, Chemical Engineering Progress 48 (4) (1952) 173–180.

[135] C. Schwellnus, A study of a general one-dimensional two-fluid critical flow model, Master's thesis, McMaster University (November 1988).

[136] R. Dagan, E. Elias, E. Wacholder, S. Olek, A two-fluid model for critical flashing flows in pipes, International journal of multiphase flow 19 (1) (1993) 15–25.

[137] S. Olek, Y. Zvirin, E. Elias, Bubble growth predictions by the hyperbolic and parabolic heat conduction equations, Wärme-und Stoffübertragung 25 (1) (1990) 17–26.

[138] D. Bestion, Extension of CFD codes application to two-phase flow safety problems, Nuclear Engineering and Technology 42 (4) (2010) 365–376.

[139] M.-S. Jin, C.-T. Ha, W.-G. Park, Numerical study on heat transfer effects of cavitating and flashing flows based on homogeneous mixture model, International Journal of Heat and Mass Transfer 109 (2017) 1068–1083.

[140] D. Labuntzov, B. Lolchugin, V. Golovin, E. Zakharova, L. Vladimirova, High speed camera investigation of bubble growth for saturated water boiling in a wide range of pressure variations, Thermophys. High Temp. 2 (1964) 446–453.

[141] M. Blander, J. L. Katz, Bubble nucleation in liquids, AIChE Journal 21 (5) (1975) 833–848.

[142] Y. Aleksandrov, G. Voronov, V. Gorbunkow, N. Delone, Y. Nechayev, Bubble chambers (translated by Scripta Technica, Inc.) (1962).

[143] I. Ansys, ANSYS CFX-solver theory guide, 2012.

[144] Y. Liao, T. Ma, L. Liu, T. Ziegenhein, E. Krepper, D. Lucas, Eulerian modelling of turbulent bubbly flow based on a baseline closure concept, Nuclear Engineering and Design 337 (2018) 450–459.

[145] S. Mimouni, M. Boucker, J. Laviéville, A. Guelfi, D. Bestion, Modelling and computation of cavitation and boiling bubbly flows with the NEPTUNE_CFD code, Nuclear Engineering and Design 238 (3) (2008) 680–692.

[146] M. Robert, M. Farvacque, M. Parent, B. Faydide, CATHARE 2 V2.5: A fully validated CATHARE version for various applications, in: The 14th

International Topical Meeting on Nuclear Reactor Thermalhydraulics, NURETH-10, 2003.

[147] Y. Liao, D. Lucas, Numerical analysis of flashing pipe flow using a population balance approach, International Journal of Heat and Fluid Flow 77 (2019) 299–313.

[148] A. K. Singhal, M. M. Athavale, H. Li, Y. Jiang, Mathematical basis and validation of the full cavitation model, J. Fluids Eng. 124 (3) (2002) 617–624.

[149] G. H. Schnerr, J. Sauer, Physical and numerical modeling of unsteady cavitation dynamics, in: The 4th International Conference on Multiphase Flow, ICMF-4, 2001.

[150] M. Ishigaki, T. Watanabe, H. Nakamura, Numerical simulation of two-phase critical flow with the phase change in the nozzle tube, Journal of Power and Energy Systems 6 (2) (2012) 264–274.

[151] T. Kuroda, T. Watanabe, Y. Kukita, Break flow modeling for a steam generator tube rupture (sgtr) incident in a pressurized water reactor (pwr), Tech. rep., Japan Atomic Energy Research institute (1993).

[152] W. H. Lee, A pressure iteration scheme for two-phase flow modeling, in: Multiphase Transport: Fundamentals, Reactor safety, Applications, 1980.

[153] L. Tikhonenko, L. Kevorkov, S. Lutovinov, Investigation of local parameters of critical flow of hot water in straight pipes with a sharp inlet edge, Thermal Engineering 25 (2) (1978) 40–43.

[154] H. Fauske, The discharge of saturated water through tubes, in: Chemical Engineering Progress Symposium Series, 1965.

[155] M. Duponcheel, J.-M. Seynhaeve, Y. Bartosiewicz, Implementation and assessment of the delayed equilibrium model for computing flashing choked

flows in a multi-field cfd code, in: The 14th International Topical Meeting on Nuclear Reactor Thermalhydraulics, NURETH-16, 2015.

[156] I. Karathanassis, P. Koukouvinis, M. Gavaises, Comparative evaluation of phase-change mechanisms for the prediction of flashing flows, International Journal of Multiphase Flow 95 (2017) 257–270.

[157] R. D. Reitz, A photographic study of flash-boiling atomization, Aerosol Science and Technology 12 (3) (1990) 561–569.

[158] Y. Liao, D. Lucas, On numerical simulation of flashing flows, in: The 14th International Topical Meeting on Nuclear Reactor Thermalhydraulics, NURETH-18, 2019.

[159] J. C. Jo, J. J. Jeong, B. J. Yun, F. Moody, Numerical prediction of a flashing flow of saturated water at high pressure, Nuclear Engineering and Technology 50 (7) (2018) 1173–1183.

[160] J. C. Jo, J. J. Jeong, B. J. Yun, J. Kim, Numerical analysis of subcooled water flashing flow from a pressurized water reactor steam generator through an abruptly broken main feed water pipe, Journal of Pressure Vessel Technology 141 (4) (2019) 044501:1–10.

[161] Y. Liao, D. Lucas, E. Krepper, R. Rzehak, CFD simulation of flashing boiling flow in the containment cooling condensers (CCC) system of kerena$^{\mathrm{TM}}$ reactor, in: 21st International Conference on Nuclear Engineering, ICONE-21, American Society of Mechanical Engineers Digital Collection, 2013.

[162] Y. Liao, C. Schuster, S. Hu, D. Lucas, CFD modelling of flashing instability in natural circulation cooling systems, in: The 21st International Conference on Nuclear Engineering, ICONE-26, American Society of Mechanical Engineers Digital Collection, 2018.

[163] D. Lucas, M. Beyer, L. Szalinski, Experiments on evaporating pipe flow, in: The 14th International Topical Meeting on Nuclear Reactor Thermal-hydraulics, NURETH-14, 2011.

[164] Y. Liao, D. Lucas, E. Krepper, R. Rzehak, Flashing evaporation under different pressure levels, Nuclear Engineering and Design 265 (2013) 801–813.

[165] S. Hänsch, D. Lucas, E. Krepper, T. Höhne, A multi-field two-fluid concept for transitions between different scales of interfacial structures, International Journal of Multiphase Flow 47 (2012) 171–182.

[166] T. Höhne, E. Krepper, D. Lucas, G. Montoya, A multiscale approach simulating boiling in a heated pipe including flow pattern transition, Nuclear Technology 205 (1-2) (2019) 48–56.

[167] T. Höhne, D. Lucas, A multiscale approach simulating generic pool boiling, Nuclear Science and Engineering (2020) 1–14.